

10 **Seismic and structural characterization of a pre-salt rifted section: the Lagoa**  
11 **Feia Group, Campos Basin, offshore Brazil**

12 **Iacopini D<sup>1</sup>, Alvarenga R. S.<sup>2</sup>, Kuchle J<sup>2</sup>, Cawood A. J.<sup>1</sup>, Goldberg K<sup>2</sup>, Kneller B<sup>1</sup>,**

13 <sup>1</sup> School of Geosciences, University of Aberdeen, UK

14 <sup>2</sup> Instituto de Geociências, BG Rift Lab, Universidade Federal do Rio Grande do Sul, Porto Alegre, Brazil

15

16 **Abstract**

17 The exploration of pre-salt offshore SE Brazil presents a multifaceted deep-water scenario that is  
18 bringing new challenges to seismic interpretation in offshore Brazilian exploration and production.  
19 Reservoirs in this domain are complex, heterogeneous with layered carbonates which makes accurate  
20 reservoir characterization very challenging. Our study here deals with the seismic characterization of  
21 the stratigraphy of a lacustrine section from the Lagoa Feia Group (Winter et al., 2007) in the Campos  
22 Basin, which extends over an area of 100,000 km<sup>2</sup>. By using an extensive 2D seismic dataset and two  
23 deep well logs and core information, we propose a seismic facies analysis and structural characterization  
24 of the Lagoa Feia group focused in the inner proximal domain of the Campos basin. Inferences from  
25 well core and seismic stratigraphy clearly suggest that the all Lagoa Feia group has a syn-rift  
26 depositional character. Different pre- syn- and post-rift seismic stratigraphic units, with corresponding  
27 bounding surfaces, are then defined. Based on their seismic character, four seismic facies representing  
28 the main lithological package in the rift section are recognized: border fault deposits; fine grain-  
29 dominated re-sedimented deposits; coarse grain-dominated carbonate rich re-sedimented deposits; and  
30 an intrusive wipe-out zone affecting all the pre-salt unit. Using some simplified kinematic restoration  
31 we show that some of the normal faults affecting the lower units of the Lagoa Feia could be interpreted  
32 as pre-rift structures *sensu lato* but also as pre-existing structures re-activated during the main passive  
33 margin rift activities. By proposing this seismic classification and interpretation across the pre salt  
34 Campos Basin units, this work represents an introductory step to a facies classification and structural  
35 interpretation applicable at regional level in the internal SE Brazil offshore area.

36 **1 Introduction**

37

38 The Campos Basin, offshore E Brazil, has an area of roughly 100 000 km<sup>2</sup> and is one of the most prolific  
39 zones of the South Atlantic, with more than 2900 drilled wells (Guardado et al., 2000; ANP-BDEP,  
40 2015). Prior to the recent discoveries of significant hydrocarbon volumes in the pre-salt intervals,  
41 suprasalt reservoir accumulations corresponded to more than 90% of Brazil's petroleum reserves

42 (Winter et al., 2007). Recent estimates (ANP-BDEP, 2018), however, suggest that 51% of total proven  
43 reserves in the Campos Basin are related to pre-salt accumulations. The Lagoa Feia Group, (Schaller,  
44 1973), contains both supratidal and upper-intertidal facies (Wright, 2012; Wright and Barnett, 2015;  
45 Herlinger et al., 2017) which provide reservoir intervals for these pre-salt accumulations, and the  
46 organic-rich lacustrine source rocks (Armelenti et al., 2016; Goldberg et al., 2017) from which  
47 hydrocarbons across the basin are derived. The Lagoa Feia Group, deposited in the pre-salt rift and sag  
48 phases of the basin evolution, thus represents an important component of the Campos Basin petroleum  
49 system.

50

51 In light of recent pre-salt discoveries in the Campos Basin, existing understanding of the Lagoa Feia  
52 Group (Abrahão & Warme, 1990) has recently been re-interpreted and refined. Detailed petrologic-  
53 sedimentologic studies (Armelenti et al., 2016; Herlinger et al., Wright and Barnett, 2015) and seismic  
54 stratigraphic approaches have resulted in interpretation of this interval as either re-sedimented  
55 gravitational deposits within a rift lacustrine environment (Alvarenga et al., 2016; Goldberg et al.,  
56 2017;) or as thicknesses of lacustrine carbonate facies in the more distal part of the margin (Muniz &  
57 Bosence, 2018). In spite of these detailed studies, and the large number of wells drilled across the basin,  
58 the depositional and structural evolution of the Lagoa Feia Group remains poorly constrained. Few  
59 (40?) of the 2900 Campos wells penetrate the Lagoa Feia Group rift section (Armelenti et al., 2016;  
60 Muniz and Bosence, 2018) and it is estimated that less than 600 m of publicly-available cored intervals  
61 exist for the Lagoa Feia Gp. across the entire basin (Goldberg et al., 2017), despite the regional  
62 importance of this interval.

63

64 This paper aims to build on existing petrographic, stratigraphic and sedimentological interpretations  
65 (Armelenti, 2016; Alvarenga et al. 2016; Goldberg et al. 2017; Herlander et al. 2017) of the Lagoa Feia  
66 Gp. by focusing on the seismic expression of the main units and structural elements within this pre-  
67 salt rift and sag interval.

68 By extracting the main seismic reflection parameters (which include geometry, continuity, amplitude,  
69 frequency) and analysing core data from two wells tied to the sub-salt seismic data, we propose several  
70 structural seismic facies that have regional significance across the Campos Basin for the Lagoa Feia  
71 Group. Based on the distribution of these proposed seismic facies and their spatial relationships to major  
72 normal faults through the pre-salt section, we explore several kinematic scenarios for the rift evolution  
73 of the Campos Basin. By comparing alternative kinematic scenarios, we discuss the significance for  
74 understanding the rift evolution of the Campos Basin.

75

## 76 **2 Geological and tectonic settings**

77 The Campos Basin, offshore Brazil, is situated on the south-eastern continental shelf part of the  
78 Brazilian offshore between the Cabo Frio High to the south and the Vitoria High to the north (Fig. 1).  
79 Like most of the Brazilian offshore basins, the Campos Basin was formed during the breakup of  
80 Gondwana and the drifting apart of South America and Africa in late Jurassic to early Cretaceous time  
81 (Mohriak et al., 2008, Karner, 2000). During this major tectonic event, both the Atlantic margin of  
82 Brazil and the west African margins experienced an extended deformation history, first involving deep-  
83 seated crustal deformation associated with Barremian-Aptian rifting, and subsequent sea floor spreading  
84 and drifting of the Atlantic margins (Mohriak, 2008). The sedimentary wedge within the Campos Basin  
85 is at least 4-6 km thick at depocenter locations, but thins locally over basement highs (Kumar et al., 1977;  
86 Zalan et al., 2011). Refraction experiments (Zalan et al., 2011; Moulin et al., 2011) suggest that to the  
87 east of the basin, the sedimentary pile overlies thinned continental crust and continental-oceanic  
88 boundary have been tentatively proposed through gravity and magnetic data analysis (Demercian et  
89 al., 1993; Zalan et al., 2011)

90 Within this tectonic framework, the sedimentary record since the Mesozoic in the Campos  
91 Basin has been traditionally described in terms of three supersequences (Winter et al., 2007, Fig. 2): (1)  
92 Rift Supersequence, (2) Post-Rift Supersequence and (3) Drift Supersequence. These supersequence  
93 classifications, as defined by Winter et al. (2007) are appraised in detail in the following sections, based  
94 on recent work and newly seismic interpreted data from the Campos Basin.

95 (1) According to Winter et al. (2007), the Rift Supersequence within the Campos Basin  
96 corresponds to basalts and minor conglomerates of the Cabiúnas Formation (Hauterivian) and the lower  
97 portion of the Lagoa Feia Group, as defined by the Atafona, Coqueiros and Itabapoana formations. The  
98 Barremian aged Atafona Formation consists of siltstones, sandstones and lacustrine shales with a  
99 distinctive talc-stevensite mineralogy (REF), and interbedded thin lacustrine limestones. The overlying  
100 Coqueiros Formation is of upper Barremian to lower Aptian age and has been described as coquina  
101 facies (“Unit D – Coquinas Sequence” of Rangel & Carminatti, 2000), but is in fact composed of  
102 rudstones and grainstones that are not located in a specific stratigraphic interval, according to Goldberg  
103 et al. (2017). The Itabapoana Formation (alluvial fans/fan deltas proximally and lacustrine/lagoon  
104 sediments distally) is also of Barremian to lower Aptian age, laterally equivalent to Atafona and  
105 Coqueiros formations (Winter et al., 2007).

106 (2) The Post-Rift Supersequence (Fig. 2) comprises the upper part of the Lagoa Feia Group,  
107 which includes the upper Itabapoana, laterally equivalent Gargau, and Macabu Formations. Overlying  
108 the Lagoa Feia Gp is the evaporitic Retiro Fm. The upper Itabapoana Fm. is dominated by marls,  
109 calcilutites and low-density turbidity current deposits, with the overlying Macabu Formation dominated  
110 by biotic/abiotic stromatolites, laminated microbialites and chemical precipitates controlled by the  
111 geochemistry of alkaline lacustrine waters (Wright 2012; Herlinger et al., 2017). The Retiro Fm., which  
112 overlies the Lagoa Feia Group, is an evaporitic sequence composed of anhydrite, carnallite and

113 halite/sylvite of Aptian age deposited in marine/lagoonal environment in an arid climate (Winter et al.,  
114 2007, Tedeschi et al., 2017 ). The upper portion of the Retiro Formation displays a retrogradational  
115 pattern, and is interpreted to represent a eustatic sea-level rise (Winter 2007; Davison, 2007). This unit  
116 marks the clear boundary between the post-rift and the underlying syn-rift (Tedeschi et al; 2017) and is  
117 remobilized into salt domes and diapirs with amplitudes of up to 3000 meters or more, which cut the  
118 overlying stratigraphy (Rangel et al. 1994).

119 (3) The Drift Supersequence comprises marine sediments of the Macaé and Campos Groups  
120 deposited in a regime of thermal subsidence associated with gravity-dominated tectonics (Winter et al.,  
121 2007), dominantly evaporite remobilization. The Macaé Group (Lower Albian to Cenomanian) consists  
122 dominantly of limestones and marls, while the Campos Group (Turonian to Recent) consists dominantly  
123 of siliciclastic sediments, deposited in progressively deeper marine environment (Winter et al., 2007).

124 In spite of these detailed lithostratigraphic classifications, particularly within the Post-Rift  
125 Supersequence, these units are not chronostratigraphically or regionally consistent, but are in fact  
126 related to specific depositional environments that varied substantially along the rift and across the  
127 Campos Basin (Karner & Gamboa, 2007; Stanton & Masini, 2013).

128

### 129 **3. Datasets**

130 The subsurface dataset (acquired through the 1980s to 1990s) consists of a series of 2D seismic surveys  
131 with a total of 282 seismic lines (but few of them have been selected here as representative), and 40  
132 wells, of which only 13 have well logs data and two have core (referred to here as wells A B, Fig. 1).  
133 Before describing the main seismic units and their tectonostratigraphic interpretation, it is worth  
134 discussing some of the properties of the seismic dataset. Most of the seismic data (2D) released for the  
135 project (Fig. 1) was acquired in the inner slope, primarily for the purpose of imaging the supra-salt,  
136 post-rift sedimentary units. They all represent pre stack time Kirchoff migrated seismic sections. As a  
137 consequence, most of the seismic processing has been focused on imaging units above the salt while  
138 only secondary attention has been paid to the sub-salt units (a coherent velocity model of the pre salt  
139 area is in fact missing). In Figure 3a, a sample of a 2D line extracted from the survey is represented in  
140 terms of the frequency. It represents a three frequency decomposition Red Green Blue (RGB) blended  
141 image (15, 35, 55 Hertz frequencies) using a constant mean frequency/ total bandwidth ratio. The  
142 blended image indicates that the highest frequencies over 35 Hz (bluish colours pointed by the arrows)  
143 are clearly associated with the supra-salt unit while the sub-salt units related to the Lagoa Feia Group  
144 are restricted to values below the 35 Hz. Using the check-shot information available within the Lagoa  
145 Feia Group (Fig 3b), which yield measured velocities varying between 2.4 and 2.7 km/sec (Fig. 3c),  
146 and using the mean frequency distribution described in Figure 3, we can estimate a minimum and  
147 maximum tuning thickness that varies between 10 and 50 m. This is the maximum resolution we can

148 thus expect in the presented seismic interpretation. Figure 3b shows the calibration of some of the major  
149 reflectors using the well log B which clearly confirms the resolution values of 10-30 m (at best),  
150 supporting the frequency analysis.

1511) The frequency analysis (Figure 3a) also suggests that the sub-salt seismic quality impaired the use of  
152 some seismic attributes to recognize and map the main boundaries between the basement (here named  
153 Cabiúnas Formation) and the main sequence. In some cases, due to the very low frequencies, the seismic  
154 resolution was well above the required tuning thickness necessary to interpret the main internal  
155 variations or lateral continuity of the seismic facies, reducing our ability to interpret details of the  
156 internal architecture of the syn-rift deposit. It is worth noting that several of the available wells were  
157 originally drilled with the intention of investigating targets located in the supra-salt sediments. This  
158 implies that most of the check-shots do not reach the Lagoa Feia Group and most of the wells do not  
159 contain any core information about the lowest pre-salt unit of interest. Only 2 wells stored useful core  
160 information across the full dataset and only two could match the entire pre-salt sequence. Another well  
161 named well C\* (Fig 1) contains well log data that have been used to calibrate some reflectors. Therefore  
162 most of our seismic facies analysis will be devoted to seismic lines that are tied to those wells (Fig. 1).

163

#### 164 **4. Methods**

165

166 Using the reflector terminations, picking the main amplitudes and using seismic attributes, allowed us  
167 to recognize the main unconformities and seismic facies. Core data from well A and B (Figs 3 and  
168 5) have been used to interpret and constrain some of the main seismic package and the seismic facies  
169 recognized. Check shot and sonic log data when available have been also used to estimate average  
170 velocities and depth convert the seismic data . data.

171

##### 1724.1 Seismic velocities

173 Interval and average velocities utilized for the seismic interpretation have been obtained mostly from  
174 both the well log, sonic log and the check shots released for this research activity. The velocities vary  
175 considerably within the different formations of the Lagoa Feia but two main packages have been  
176 recognized. The unit directly below the salt unit, across the main upper syn-rift unit, records interval  
177 velocities that vary between 2.1 to 3 km/sec. The second package, with an average velocity of 2.4 to  
178 2.5 km/sec, is defined through two interval velocities of 2.4 (upper part) and 2.5 km/sec (fig 3c) which  
179 occurs directly below the main thick redeposited carbonate rich units as, suggested by the two check  
180 shots velocities indicated in figure 3c (and white values in figure 3b). These two packages are

181 approximately delineated in figure 3c. respectively by the two bold thick lines in light orange and pale  
182 blue. Those two average of velocities has been used to calculate the mean depth across the wells.

#### 183 4.2 Seismic attributes analysis

184 In order to recognise patterns across the seismic dataset, different complex attributes (*sensu* Taner &  
185 Sheriff, 1977) and attribute combinations have been applied. Specifically the use of some attributes,  
186 such as the sweetness (specially to highlight the rift basement/first infill), the reflection strength, cosine  
187 of the phase, and relative acoustic impedance, have been crucial to resolve some of the internal seismic  
188 expression representing the main units of the Lagoa Feia. Before describing the main seismic facies  
189 recognized in this study, we will first briefly describe the various attributes utilized and outline their  
190 utility in resolving signal properties during seismic facies analysis. A summary of their properties and  
191 image visualization across the Campos Basin seismic data analysed is proposed in Figure 4.

192 1) Cosine of the phase (Taner & Sheriff, 1977): The instantaneous phase is defined as the  
193 tangent of the argument of any complex signal. The cosine of phase strictly derives from  
194 it, as it represents the cosine of the instantaneous phase. This attribute is of central  
195 importance, since it describes the location of events in the seismic trace and leads to the  
196 computation of other instantaneous quantities. It also makes strong events clearer and is  
197 effective at highlighting discontinuities of reflectors, faults, pinch-outs, angularities and  
198 bed interfaces. Seismic sequence boundaries, sedimentary layer patterns and regions of  
199 onlap/offlap patterns often exhibit extra clarity by using this attribute.

200 2) Root mean Square amplitude (Taner & Sheriff, 1977): we define the RMS as the root mean  
201 square amplitude of the signal (also known as “instantaneous amplitude or envelope”),  
202 calculated by taking the root of the summation of the squared real components of the signal.  
203 It is similar (but analytically not equivalent) to the RMS amplitude as it highlights, by doing  
204 the square rooted amplitude, the various anomalies within the seismic datasets. RMS is  
205 amplitude independent of phase attributes, it is always positive, and has the same range of  
206 squared values as the amplitude from which it is derived. To appreciate the main  
207 description and effect refer to the table in Figure 4.

208 3) Relative acoustic impedance (RAI). The relative acoustic impedance (called here RAI) was  
209 proposed by Chopra et al. (2009) and is the result of a simple integration of the complex  
210 trace. To calculate it first we invert the seismic amplitudes into a reflectivity series using  
211 spectral inversion. Then we transform this reflectivity series into a relative impedance  
212 layers. This step is a trace-by-trace calculation process. It basically represents the  
213 approximation of the relative acoustic impedance at high frequency components. In our  
214 study it was extremely effective in highlighting the seismic textures of the various subunits  
215 recognized and mapped within the Lagoa Feia Group.

## 216 **5. Results**

### 217 **5.1 Seismic sequence stratigraphy and regional mapping**

218 The first approach of our seismic characterization consisted of identifying the main regional seismic  
219 surfaces, with the aim of mapping the major seismic units using reflection terminations and sequence  
220 stratigraphic principles. Here we constrain the seismic interpretation of the main seismic units to the  
221 large-scale, extensional structural elements observed in the seismic lines (Figs. 5). This first approach to  
222 analysis therefore simplifies the conceptual interpretation of the area by emphasising the importance  
223 of structural-stratigraphic interactions. Here we paid specific attention to the pre-salt rift basin deposits  
224 and their relation to the main rift structure by subdividing the stratigraphy into genetically related units  
225 – systems tracts, as originally defined by Brown & Fischer (1977) but following the methodology  
226 proposed in the North Sea by Prosser (1993). A discussion and integration of the various seismic  
227 stratigraphic units and a chronostratigraphic chart of the basin locally utilized here for the Campos Basin  
228 has been presented elsewhere (Ene et al., 2015; Goldberg et al., 2017), and are outwith the scope of this  
229 study. The main seismic units and related surfaces that have been recognized and mapped are the  
230 following (Fig. 5; see Fig. 2 for stratigraphic framework):

#### 231 4.1 Pre-rift unit

232 This is the deepest seismic unit of the framework (Figs. 2 & 5) and consists of Pre-Cambrian plutonic  
233 and metamorphic rocks (Goldberg et al., 2017). The seismic reconnaissance of the pre-rift unconformity  
234 is precluded due to (1) its deep occurrence (over 8km), and (2) low acoustic impedance contrast between  
235 these crystalline basement rocks and the basalts of the syn-rift section, with their low frequency  
236 characteristic (Fig 3A). The majority of information regarding this deep section comes from well core  
237 and log data which were used to tie and calibrate the main seismic units, and the response of this section  
238 to sweetness attributes. Here we refer to three main seismic lines (sections A, B and C; Fig. 5) and the  
239 two main wells used in this study: well A and well B(see Fig. 1 for locations of seismic lines and wells).

240- Top Cabiúnas Formation: The well data (the purple unit in well B in Figs. 5A, and 5b and well A in Fig  
241 5C) characterize the Cabiúnas Formation as sediments inter-fingered with thin basalt sills (Goldberg et  
242 al.,2017). The top of the Cabiunas formation represents a lithological contrast between the basalts and  
243 the overlying sediments, with no chronostratigraphic significance (Goldberg et al.,2017). The top  
244 Cabiunas formation is represented as a red dashed line (Figs 5a to c, 8 to 10). The top of this unit is only  
245 clearly mappable by using the wells and a combination of amplitude- and phase attributes (Fig 4) that  
246 helped to enhance the very low impedance reflection (see Fig. 5b). Using the well tie information, the  
247 Top Cabiúnas Formation appear defined by a very discontinuous reflection marked by a red dotted  
248 interpretation (Fig. 5a-c). This reflection doesn't show any real lateral continuity, which may be  
249 suggestive of a non-planar interface between this interval and the overlying deposits. As shown in all

250 the seismic lines (Figs. 5), the Top Cabiúnas Formation is also extensively offset by several extensional  
251 faults through the seismic sections (white faults, figs 5a-c).

252-

## 253- 5.2 Syn-rift unit

254- Above the top Cabiúnas Formation a thick syn-rift unit, characterized internally by two main  
255 discontinuities, has been systematically mapped and recognized across all the seismic lines in the sub-  
256 salt rift basin. The base of this unit is defined by the top of the Cabiúnas Formation, while the top of the  
257 entire unit is defined by a *pre-salt Unconformity* (reflection highlighted as bold red in Figs. 5a,b and  
258 c), which consists of an intense erosional truncations observed across the entire rift basin. The real  
259 significance of this unconformity will be further investigated and questioned in the following paragraph.  
260 As stated above, using seismic stratigraphy criteria this syn-rift unit has been subdivided into three  
261 additional sub-units using internal reflection termination and geometry.

262- **Subunit 1:** This unit represented by the pre-rift package above top Cabiunas horizon. The reflectors  
263 characterizing this subunit are very difficult to interpret due to their low resolution and poor contrast of  
264 impedance. However some characteristic reflector terminations can still be observed and help to  
265 understand the initial rift depositional history respect to the small scale rift fault. As shown in figure 5b  
266 the reflections above the Cabiunas formation the following characteristics :

267- a) the reflectors) are mostly parallel and onlapping to the rift faults (Fig. 5a, sub-section 1; fig 5b,  
268 subsection 1; fig 5c sub-section1) or truncated by the faults (fig 5a, sub section 2; fig 5c sub-section2)  
269 slightly diverging / conformable to the top Cabiunas but onlap the faults.

270- b) Within some of the internal small rift half graben the first reflector above the top Cabiúnas (Fig. 5c,  
271 sub-section 2, see dotted lines) show a slightly fan thickening relation with some of the rift faults. The  
272 reflection termination against the faults in some case are unclear or chaotic (fig 5b sub-section 2 ; fig5c  
273 sub-section1).

274- c) very low amplitude and lateral continuity with a conformable parallel reflector geometry to the top  
275 Cabiunas , but dissected by the faults (Fig 5a, sub section 2; Fig. 5b, sub-section 1 and 3).

276- Above those generally conformable reflectors we observe a second unit with a clear distinctive reflector  
277 geometry that we will call subunit 2.

278- **Subunit 2:** This second subunit represents the principal syn-depositional half-graben structural pattern  
279 expressed as a clear lateral thickening with respect to the main large listric fault, with a strong amplitude  
280 and divergent reflection pattern along the half-graben structures (Figs. 5). We have defined the  
281 regionally mapped surface that separates Subunit 1 and Subunit 2 here as a orange dotted line. (Fig. 5,  
282 orange dashed line).

283- **Subunit 3:** this third subunit is stratigraphically positioned above the subunit 2 and is characterized by  
284 a decrease in the divergence of the depositional reflectors, with dominance of wavy and parallel  
285 reflections, and lower displacement of the border faults, indicating a reduction in tectonic activity. The  
286 surface separating the sub-unit 3 from sub-unit 2 has been mapped as a continuous blue line The top of

287 sub-unit 3 is defined by a red bold surface here named the (*pre salt base*) *post rift Unconformity* (in red  
288 in Figs. 5 and 8 and 9) as it lie below the salt unit.

289- **Subunit 4:** this subunit is defined at bottom by the *post rift unconformity horizon* and at the top by the  
290 base salt (Fig. 5, green bold line). It is characterized by thinning out horizontal versus slightly divergent  
291 reflectors. It is un-affected by fault displacement. On top of this unit we define a pre-salt base  
292 unconformity (or simply salt based represented in green) that define an intense erosional truncation  
293 observed and mappable across the entire basin analysed.

294-

### 295- 5.3 Post-rift unit

296- As clearly indicated in Fig 5c, outside the mini syn-rift basin bordered by the main syn-rift fault system,  
297 subunits 1 and 2 between the top Cabiúnas Formation and the *post rift unconformity* thin out, or are  
298 strongly reduced/eroded.

299-

### 300- 5.4 Structural elements

301 As shown in the large seismic section in Fig. 5a, the deposition of the Lagoa Feia group pre-salt subunits  
302 is controlled and defined by a series of normal faults. alternating with half-grabens where the main  
303 boundary fault develops, which affects the all subunits 1, 2, part of 3. A closer look at the mapped  
304 normal faults (with red numerations in figures 5 a, b) is proposed through the figures 5a to c  
305 representing respectively the seismic line named A, B and C in figure 1. The all seismic lines are  
306 biased by a vertical exaggeration of 3:1.

307- Figure 5a shows a complete section of one of the half grabens.. The half graben structure is controlled  
308 by three different oriented fault systems: high angle fault with an antithetic orientation (fault 1 red)  
309 with respect to the low angle faults; low angle, small displacement normal fault (fault 2 in red) affecting  
310 the base of the Lagoa Feia and the top Cabiunas formations; and the large-offset listric fault (fault 3  
311 red) which controls the main graben geometry. Timing of fault populations will be further investigated  
312 through a restoration model but the geometry and the relationship with the stratigraphy indicate that the  
313 three different fault systems were all active during the half graben units 1 and 2 structuration. The low  
314 angle fault (fault 2) localized in the low part of the Lagoa Feia appear to have been the triggering  
315 structure of the first rift structuration (as by the onlapping reflection termination described, Fig. 5a, sub-  
316 section 1; fig 5b, subsection 1; fig 5c sub-section1). In some other cases the lower Lagoa Feia units do  
317 not have reflector terminations with a clear relationship (fig 5b sub-section 2 ; fig5c sub-section1) or  
318 they seem to be cutted by the faults (Fig 5a, sub section 2; Fig. 5b, sub-section 1 and 3) suggesting a  
319 later displacement. The fault system 1 (red number) are high angle normal faults and appear to cross  
320 most of the Units 1 and 2 of the Lagoa Feia formation, with an opposite dipping direction respect to the  
321 fault population 2. This is clearly observed in all the seismic lines represented in figures 5a to c,  
322 confirming the syn-rift nature of the Lagoa Feia depositional unit.

323- The reflection terminations and cutting relationship suggest that the fault population 1 has been active  
324 for longer and probably represents a later stage with respect to the fault system 2; the fault population  
325 3 is defined by a low angle listric-type of fault (fault 3 red). It clearly displaces the top Cabiunas  
326 formation by several hundred of meters (see wells A and C represented in Fig 5a) and is systematically  
327 bordered by a chaotic seismic facies where the lateral thickening Unit 2 interrupt its reflector  
328 terminations (Fig 5a to c). The fault is draped by the *pre-salt post-rift unconformity* that in all seismic  
329 lines appears unaffected by any visible displacement (figs 5).

330

## 331 **5.6 Seismic facies**

332 The main seismic interpretation and seismic image analysis consisted in recognizing the seismic facies  
333 that are repeatedly observed within the various systems tracts observed and recognized. The seismic  
334 facies are here defined through a combination of reflector geometry (using both continuity and  
335 reflection termination), waveform properties as the five seismic attributes appearance described so far  
336 (table in Figure 4). Specifically the use of the cosine of the phase, combined with mapping of the  
337 reflection terminations, proved very useful and efficient in highlighting both the thin bed, and the  
338 continuity between various reflectors. To further fine-tune the internal facies we also extracted seismic  
339 attributes related to the relative amplitude and contrast of impedance, such as the reflection strength and  
340 RAI. We then linked the various facies to their position within the fault related sub-basin to predict the  
341 environments of deposition that controlled the types of deposits (e.g. to differentiate carbonates from  
342 sandstones and mudstone units).

343 Seismic facies 1: this seismic facies is defined by chaotic and/or low amplitude reflectors (Figure 6),  
344 with no clear internal stratigraphy, often inferred to be strongly damaged by small faults and fractures.  
345 The seismic package characterized by this facies is observed mostly across the syn-rift units and is  
346 systematically juxtaposed to fault planes (Fig 5 a to c, Figs 8-10).

347 Seismic facies 2: This seismic facies (see Figure 6) is characterized by thinly layered, semi-continuous  
348 strong to medium amplitude reflections. This facies is best observed through the RAI attributes (Fig. 7)  
349 that enhance the discontinuous character as it has a granular and dotted signal in clear contrast with the  
350 surrounding facies 3. The cosine of phase expression of the texture confines the thin and non-continuous  
351 phase character of the reflectors (Fig 7b). This seismic facies is systematically observed across all syn-  
352 rift units (high to low system tract), and characterizes the package with an onlapping and slightly lateral  
353 thickening geometry (FigS 8-11).

354 Seismic facies 3. This seismic facies is observed throughout the Lagoa Feia unit between the top  
355 cabiunas formation and the post rift unconformity scattered across the half graben basin. It is  
356 characterized by very continuous, thick and strong reflections, interbedded with or even floating within  
357 the thinly-layered seismic package (seismic facies 2). The seismic character is better represented by the

358 RAI attributes, highlighting strong continuous and bright reflectors (Fig. 7a). Similarly the cosine of  
359 phase shows quite thick and continuous reflectors (figure 7b). The packages show quite abrupt  
360 boundaries, but do not show any onlap or lateral thickening. They appear as the brightest and distinctive  
361 reflectors of the pre-salt units.

362 Seismic facies 4. A fourth seismic facies (Fig. 6) is characterized by a wipe-out zone where the seismic  
363 reflections are strongly disrupted, affected by low amplitude, and pull-ups typical of intrusive features.  
364 This seismic character crosses all of the Lagoa Feia connecting the Cabiúnas Formation, reaching the  
365 base of the salt and pre salt unconformity, suggesting a late/post depositional event with respect to  
366 rifting. For an extensive analysis and discussion of those feature in the pre salt campos basin we refer  
367 to Alvarenga et al (2016).

368 The seismic facies recognized has been then mapped across the seismic lines B,C and A using the  
369 proposed classification (Figs 6 and 7) and the results will be shown respectively in Figures 8, 9 and  
370 10 (the numbers 1 to 3 represent the seismic facies described above). The dotted lines represent the  
371 boundaries of seismic facies 3.

## 372 **5.7 Correlation of seismic facies to well data**

373 Seismic image analysis of individual units recognized through their facies response can potentially  
374 improve our understanding of the volumetric distribution of the various lithological units, and prepare  
375 the ground for future reservoir characterization of the sub-salt Lagoa Feia units. Brown & Fisher (1980)  
376 defined seismic facies as the expression on seismic reflections of geological factors that generate them,  
377 such as lithology, stratification, depositional features, etc. Therefore although we are lacking a robust  
378 well log calibration of seismic facies we matched the seismic facies with the two available wells (called  
379 here well A and well B ) after time-converting them using checkshots/socic logs information. Two of  
380 these well data (Well A and Well B) represented the only geological and petrophysical constraints  
381 available across the mapping area. They have been part of the dataset used to define the main  
382 petrography and sedimentology background by Armententi et al (2016) and Goldberg et al (2017). Well  
383 C has no core available but had useful well log information to correlate the top Unit 4 across the seismic  
384 dataset (Fig 5a). We first briefly describe below the main stratigraphical information obtained from the  
385 three wells (Fig 11 for a description), and then use it to define the main seismic units matching the  
386 seismic facies mapping analysis.

387 As shown in Figures 8 to 10, wireline log data and continuous core information from two wells (well A  
388 and B) have been used to assess the seismic facies recognized within the Lagoa Feia, and assign them  
389 a geological significance. A legend describing the main lithological units representation is proposed in  
390 figure 11 using the Well B (Fig 11). A detailed petrographical, petrological and sedimentological  
391 description of these cores is given by Armententi et al. (2016) and Goldberg et al. (2017). Here we use  
392 only the main lithologies for calibration purposes, to constrain and interpret the main seismic facies.

393 Well A (Fig 8) extends to some distance below the salt, and penetrates the pre- and syn-rift deposits.  
394 Well B is instead represented in figures 9 and 10. The section crossing the main facies 2 and 3 has been  
395 zoomed in Fig 11. Well C contain information only for the shallow post-rift pre salt part of the Lagoa  
396 Feia Group (Unit 4) flanking the half graben minibasin.

#### 397 5.7.1 Well A

398 Well A (Fig. 8) tying seismic line C: well A shows three main package of unit part of the high and low  
399 stand system tract. The enclosed white numbers, indicate the seismic facies and the black dotted lines  
400 marks their distribution across the syn-rift units. A first package (yellow bracket) just below the red  
401 bold line unconformity characterized by semi-continuous, thinly layered reflections of low amplitude  
402 defined by a complex alternation of thick units of sandstone and shale/mudstone the seismic facies  
403 correspond to the seismic facies described as 2. A second package placed within the lateral thickening  
404 reflectors and characterized by a strong correspondence of the “fat and bright” reflectors (described as  
405 seismic facies 3) matching with the occurrence of very finely layered units characterized by alternation  
406 of coarse-grained limestones, calcilutite with mudstone / shale and the Coquinas unit (see the yellow  
407 brackets indicating the marl/S limestone units). A third package bounded between the second package  
408 and the Cabiúnas formation is characterized by similar semi-continuous, thinly layered reflections of  
409 low amplitude as the first package. This package is characterized instead by an alternance of thick  
410 conglomerate unit with shale units and thin layer calcarenite. This seems to suggest that the bright and  
411 thick reflections are associated with the presence of coarse-grained limestones within the Lagoa Feia  
412 Group.

#### 413 5.7.2 Well B

414 Well B (Figs 9, 10 and magnified version in Figure 11) tying seismic lines A and B: this well penetrates  
415 through the Lagoa Feia Group depositional units at a more proximal position respect to the large scale  
416 listric fault. This unit is slightly more condensed and the bottom part slightly penetrates the Cabiúnas  
417 Formation. Again a similar sequence of packages to well A (from top to bottom) can be recognized  
418 (refer to Fig 9). A first package located mostly in the upper part characterized by a seismic facies of the  
419 type 2 tying mostly an alternation of thick units of sandstone and shale/mudstone. A second package  
420 defined mostly by a seismic facies of type 3 mostly confined again within the lateral thickening fat and  
421 bright reflectors and characterized by alternation of coarse-grained limestones, calcilutite with  
422 mudstone / shale and the Coquinas unit. A third package is again extremely similar to what has been  
423 described with the well A where seismic expression is defined mostly by the seismic facies 2  
424 characterized by the alternance of thick shale, conglomerate units and thiny calcarenite. Therefore well  
425 B confirms similar relations described by the well A, where the presence of dense coquinas and  
426 calcarenite is clearly marked by fat and bright reflections in a lateral thickening package associated with  
427 seismic facies 3 across the entire unit. In both case the basalts (in the pre/syn rift units) of the Cabiúnas

428 Formation do not generate any real contrast of impedance, possibly due to the absorption effect of the  
429 high frequency component of the signal of the above layered limestone subunits.

430 None of the two wells adds any information about the seismic facies 1, as they do not intersect the  
431 associated unit. All the seismic sections imaging the deep rift structure represented in Figures 8, 9 and  
432 10 indicate that the chaotic and low amplitude seismic texture without any internal stratigraphy  
433 recognized here as seismic facies 1, are systematically juxtaposed to small or large fault bordering the  
434 small sub-basin underlying the sag and salt unit.

## 435 **6. Discussion**

### 436 7.1 Interpretation of the Lagoa Feia seismic stratigraphy

437 The detailed sedimentological analysis obtained from well correlation of our area of interest, have been  
438 proposed in previous companion paper by Goldberg et al. (2017) and indicates that the absence of clear  
439 retrogradational or progradational stacking patterns suggests a dominant intrabasinal depositional  
440 system, mostly controlled by the small normal and border fault. Our seismic description indicates that  
441 all the major seismic units and structure described in the Lagoa Feia formation are deposited within a  
442 setting mostly controlled by an active tectonic expressed through the normal high angle faults and the  
443 large border fault bounding asymmetric graben. This allow us to interpret the reflector geometry and  
444 their internal facies characteristics described, within a depositional system dominated by the tectonic  
445 control with poor input from extrabasinal system. Therefore for the seismic interpretation of the Lagoa  
446 Feia subunits (refer to Figs. 2 and 5 ), we adopted the criteria and scheme proposed by Prosser (1993)  
447 and Norverdt et al. (1995) following their proposed tectonic system tracts.

- 448 - The first subunit has been described as concordant to or onlapping both the small normal block  
449 faults (fault system 2, involving mostly the basement units) and to the chaotic seismic facies  
450 bordering the large listric fault structures (fault system 3) controlling most of the tectonic  
451 subsidence; In a rift related linked depositional system, those succession roughly correspond to  
452 the rift initiation starting with an early syn rift unconformity sensu Prosser (1993) and Norverdt  
453 et al (1995). Following the terminology by Prosser (1993) we refer to the first unit as the *Rift*  
454 *Initiation Systems Tract*, which is stratigraphically comprised between the top Cabiúnas  
455 volcanics (dotted red) and the first lower lateral thickening reflection of the Lagoa Feia called  
456 *Half graben development surface* and mapped as a dotted orange reflector.
- 457 - Above the *Half-Graben Development Surface* is deposited the second subunit. It shows an  
458 aggradation, lateral thickening (versus the listric fault) and then draping the *Rift Initiation*  
459 *Systems Tract* but laterally onlapping the main boundary faults (system 3) or the product of the  
460 scarp degradation, always confined within individual half-graben systems. The reflectors all  
461 terminate more or less abruptly against the chaotic facies 1, bordering the listric fault controlling  
462 the geometry of the asymmetric graben. They clearly represent the early and later onset of the

463 rift climax where subsidence controlled by the fault activities is still faster than the  
464 sedimentation. As a consequence those units are comparable with what Prosser (1993) calls the  
465 units sequence of early - mid climax syn rift and are certainly part of the syn rift megasequence  
466 of Winter (2007). As the geometry of those reflectors is mainly controlled by the listric faults  
467 and affected by late high normal faults we call that unit as the *High Tectonic Activity Systems*  
468 *Tract*.

469 - The third subunit is again draping and transgressing the previous unit and still downlapping to  
470 onlapping (in places) the large chaotic facies bordering the boundary faults across the small  
471 half-graben at a more regional scale. It is bounded at the bottom by the *Maximum rifting*  
472 *sequence (blue line)*. As the reflector clearly show a reduced lateral thickening (but still  
473 downlapping the chaotic zones close to the footwall scarp) we suggest that unit may represents  
474 the late rift climax (sensu Prosser, 1993) where the listric fault activity start to decelerate  
475 leading to the first immediate post rift succession through an intermediate late *pre salt post rift*  
476 *unconformity (red)*. This pre salt top unconformity is probably locally equivalent to the pre  
477 Alagoas transitional megasequence (Guardado et al, 1990; Karner, 2000) but better  
478 chronostratigraphic data are needed to support this interpretation.

479 - Finally we observe the subunit 4 that appear totally unaffected by the listric fault and the re  
480 activated high normal fault. It may be interpreted as *late post rift system* sensu Prosser  
481 (1993).  
482

## 483 6.2 Seismic facies & structural characteristics

484 The workflow and seismic characterization proposed here allowed us to map and reconstruct the main  
485 pre salt units structures and interpret the seismic facies of the major subunits of the lower Lagoa Feia  
486 Group. Due to the particular position of the lower Lagoa Feia, sandwiched between the salt unit above  
487 and the basalt below, in a present-day deep water location (1 to 2 sec TWT), the quality of the seismic  
488 data over the main sequence and sub-units is low and the vertical resolution is limited to the tuning  
489 thickness (10-30 m) producing large uncertainty. Most of the high frequencies are in fact absorbed by  
490 the salt and partly by the main calcarenite, calcilutite and coquinas-limestone units (Fig 3a). Moreover  
491 the seismic properties observed indicate the pre/syn-rift units constituted by basalt and interlayered  
492 shale (Cabiúnas Formation and lower portion of the Lagoa Feia Group) are rendered almost invisible,  
493 or characterized by very weak reflections. The basaltic units are in fact inferred mainly through well  
494 bore and well log information but cannot be traced out through a clear amplitude seismic distinctive  
495 response. This could suggest that within the Cabiúnas Formation the thin-bed character of the  
496 interlayered basaltic intrusion is probably producing an extremely damaged or poor signal, certainly  
497 hiding more complex relationships than simple layering structure as various other authors has suggested  
498 (Magee et al.,2015).

499 As a consequence our attention has been here focused on the above seismic package part of *the rift*  
500 *initiation tract, high tectonic activity systems tract, late rift system tract* and the post rift units all  
501 stratigraphically above the Cabiúnas Formation. Using limited well log and core information to calibrate  
502 their seismic waveform properties, three major seismic facies (facies 1, 2 and 3) have been recognized  
503 and associated with three different lithological units characterizing the Lagoa Feia Group (Figure 9). In  
504 figurews 8, 9 and 10 representing respectively the seismic line CA, A and B (with a different vertical  
505 exaggeration respect to Fig 5) the facies are numbered by the white number enclosed in the round box.

506 1) The units associated with seismic facies 1 show chaotic reflectors, without continuity (see the  
507 yellow area in Fig 12) and with low average amplitude. Its occurrence is geographically associated  
508 with the border faults, suggesting that their deposition is controlled by the fault movement (Figs 8  
509 , 9 and 10 ). This facies seems never to occur within the earliest syn-rift deposit, probably because  
510 there was insufficient topographic relief at this time to form the deposit. Across the all lines, the  
511 unit shows also marked amplitude discontinuities, often intersected by small faults, producing a  
512 dotted signature of the signal. The seismic character, location and geometry all suggest the deposit  
513 may be related to a range of hanging-wall collapse mechanisms. Collapse of the hanging-wall to  
514 the main listric fault (Fault 3 in Figs 5A to C) may be attributed to listric fan formation during  
515 extensional faulting (Gibbs, 1984) and associated rock fall, debris flow and sediment slumping  
516 processes (Prosser,1993). Similarly, recurrent extensional pulses along this border fault (Fig 5a-c  
517 and Figs 8-10) may have remobilized shallow-water sediments and allowed gravitational mixing  
518 and re-deposition of both pre-rift footwall and syn-rift hanging-wall material (Goldberg et al.,  
519 2017). Therefore facies 1 is interpreted as breccia and re depositional slope deposits originated  
520 from erosive mechanism along the fault edge due to the displacement increase of the footwall block  
521 right after its failure. They are commonly interpreted as conglomeratic deposits, named as border-  
522 fault deposits (Goldberg et al, 2017).

523 2) Seismic facies 2 (Figs 8-10) shows instead a diverging configuration across the majority of the sub-  
524 basin analyzed, suggesting a hummocky configuration in the depocenter across all the half-grabens  
525 examined (Figures 8 to 10). The shale/marl and thick sandstone units that compose the facies unit  
526 2 are characterized by the absence of coquinas or other carbonates. They affect both unit from the  
527 initial rift system tract as much as the upper part of the High tectonic system tract and the tectonic  
528 change surface.. This facies is rather characterized and controlled by the thick layered and low  
529 amplitude continuous reflectors (Figs 5 and 6 and 8 to 10). According to the well data, and to the  
530 existing petrographical information (Armelenti et al., 2016; Goldberg et al., 2017), facies 2 can be  
531 linked both to the Barremian aged Atafona Formation consisting of siltstones, sandstones and  
532 lacustrine shales with a distinctive talc-stevensite mineralogy, interbedded thin lacustrine  
533 limestones as to the Itabapoana Formation (alluvial fans/fan deltas proximally and  
534 lacustrine/lagoonal sediments distally) but also the lower Aptian age, partly laterally equivalent to

535 the Macabu formation characterized by laminated microbialites and chemical precipitates  
536 controlled by the geochemistry of alkaline lacustrine waters (Armelenti et al., 2016; Erlinger et al  
537 2017). The two units have been interpreted by Goldberg et al. (2017) as fine-grained lake sediments,  
538 associated with sediment gravity flow deposits.

539 3) Seismic facies 3 shows reflections with a rather parallel configuration, but with an average high  
540 amplitude and good continuity, producing a rather tabular geometry (Figs 5 and 6, 8-10). As shown  
541 in Figure 5 they show the highest frequency response within the *Hightectonic system tract*. The  
542 reflector terminations seem to indicate onlap geometry characterized also by some structural  
543 truncation. The facies 3 is usually dispersed or sandwiched within the facies 2 (Atafona and  
544 Itabaquana formations equivalent), and can occur both along the basin margins as well as in the  
545 depocenter of half-grabens (Figs 8, 9 and 10). This facies has been interpreted, using the existing  
546 well log information and petrographical information (Armelenti et al. 2015; Goldberg et al., 2016),  
547 as re-deposited rudstone/grainstone carbonate units, which are locally arranged in the form of  
548 mounds, and laterally shading into texture 2. Some authors such as Abrahão & Warne (1990) and  
549 Rangel & Carminatti (2000) state that the deposits of thick carbonate can be interpreted as shallow  
550 marine deposits. However, due to its scattered location, texture 3 is here interpreted as a result of  
551 reworking and erosion of a shallow bank. The deposits associated with this seismic facies have been  
552 here named as coarse grain-dominated re-sedimented deposits (Goldberg et al., 2017).

553 4) A fourth seismic facies shown in Figure 8 indicates an intrusive feature, characterized by a large  
554 wipe-out zones with some pull-up velocity effects enhanced (possibly exaggerated by an incorrect  
555 velocity model) affecting the entire Lagoa Feia Group and touching the sag unit. This feature has  
556 not previously been described, but its geometry and texture suggest that important gas chimneys  
557 affect the entire pre-salt unit. The nature and significance of this structure has been extensively  
558 described in the companion paper by Alvarenga et al (2016).

559 The distribution of the recognized facies across two analysed seismic lines are shown in figures 8 (Line  
560 C), 9 (Line A) and 10 (line B) through the white numbers. A full colour representation of the main  
561 facies is shown in Fig 12 and it clearly indicates the scattered nature of the main re-deposited units within  
562 the layered and low amplitude facies characterizing the top and bottom unit.

### 563 **6.3 Structural considerations and kinematic restoration test**

564

565 The seismic mapping of the Lagoa Feia Formation (across the seismic lines A, B and C) allowed for a  
566 clear description of their stratigraphic relationship with the syn-rift faults. All of the structures and  
567 reflection terminations observed (Figs 5) suggest that the Lagoa Feia Formation was deposited during  
568 a punctuated tectonic extension, when certainly faults populations 2 and 3 (red numbers) were active  
569 and displacing (Figs. 5a and 5b). Cross-cutting relationships also show that the W-dipping faults in the

570 western parts of Lines A and B (Fault Set 1) post-dating the deposition of the upper part (high to tectonic  
571 change surface) of the Lagoa Feia Fm and thus suggest a stage of extension that post-dates that of faults  
572 set 2 and Fault set 3. Due to poor resolution and the degraded nature of the seismic data, particularly  
573 in the hanging-wall to Fault 3 (Seismic Facies 1), and in the lower part of the Lagoa Feia Formation  
574 (Seismic Facies 2), refinement of structural models, and a determination of relative fault timings (of  
575 Fault Set 2 and fault 3) has not been possible. Therefore two problems still remain of limited solutions:  
576 Bedding geometries (and their reflector terminations) of syn-rift deposits in the initial units of the Lagoa  
577 Feia Formation are poorly constrained and thus do not provide a definitive solution to relative fault  
578 timings. The lack of clearly defined seismic horizons in the hanging-wall of Fault 3, particularly  
579 adjacent to the fault, does not allow for estimates of syn-rift deposition rates. Seismic mapping of the  
580 Top Cabiúnas and its relation with the extensional faults in the lower part of the rift initiation system  
581 track however, does not provide an obvious relative timing between the Fault Set 2 and Fault set 3 -  
582 whether movement on these faults were synchronous or one population pre-dated the other.

583 Similarly, the presence of listric fault roll-overs or synthetic fans cannot be deduced from the available  
584 data (Gibbs, 1983). Thus, the nature of the seismic expression does not provide sufficient data for robust  
585 kinematic restoration and a definitive relative timing for Fault Set 2 and Fault 3 but clearly does not  
586 exclude kinematically their mutual activities.

587 Therefore a simple restoration approach applied to Seismic Line A, which retains line lengths of key  
588 reflectors (Fig. 13), helped to explore and clarify some of these aspects. Two scenarios have been  
589 investigated.

590 A Scenario 1 (Fig. 13 a to d) in which the E-dipping faults are kinematically linked and coeval to the  
591 large listric fault.

592 A scenario 2 (Fig. 13 ), in which E-dipping normal faults which deform the base of the Lagoa Feia  
593 Formation, the Cabiúnas Formation, and underlying deposits, before the onset of fault movement along  
594 the large W-dipping listric fault.

595 As indicated in Figs 13 b and 13 c both scenarios, when restored, produce very similar results and in  
596 both cases can lead to a final restorable structure similar to those mapped in Seismic Line A (Fig. 13d).  
597 Essentially the following kinematic evolution can be proposed:

598 An initial extensional rift event where the low angle small rift fault are active (or re-activate pre existing  
599 structural high) and create the small rift structure with syn depositional structure which geometry and  
600 architecture correspond to the Rift initiation system track (Fig 13 b). At a certain point the stress field  
601 condition produces some strain localization where one of the small west dipping faults start to localize  
602 the extension (Figs. 13 c to d) producing a large listric fault (Fig. 13d) that will control the main half  
603 graben structure. That listric fault will produce the main conglomerate breccia and reworked deposit

604 observed in all the seismic lines (Figs. 8 , 9 and 10) and described as seismic facies 1 (Fig. 6) . The  
605 system will continue till the extension will relax or decelerate or till the stress field will re orient  
606 activating new extensional fault population aside of the main basin (Fig. 13 e).

#### 607 **6.4 Structural evolution**

608 The simple kinematic test coupled to the seismic mapping across three seismic line A to C (driven by  
609 the three well data analysis) helped us to reframe and define the structural characteristic of the Campos  
610 pre salt structure in the area of investigation. The rifted half graben basin where most of the re-  
611 depositional system has been described and here investigate show a story characterized by west dipping  
612 low angle fault initially triggering the main extension , affecting the top Cabiúnas Formation and  
613 creating the initial space for the first Lagoa Feia unit (Fig 13 a to c). Those fault seem to remain active  
614 during the enucleation and main displacement activity of the large listric fault (Fig. 13 d to e) that will  
615 shape the final half-graben structure and allow for the major unit of the Laoga feia to be deposited and  
616 preserved so far. During the deposition of the mid-upper unit of the Lagoa Feia (High to Tectonic  
617 change system tract) the rift system seem to still be active and probably affected by a different stress  
618 orientation that re activate or enucleate east dipping fault (fault system 3 in Fig. 5a and Fig. 13 d). Those  
619 two fault systems will contribute to create the syncline type half graben system observed across the  
620 Campos Basin. Different cross section, represented in Fig.14, seem to confirm that trend and that overall  
621 geometry: from the different seismic line crossing along the extension (Fig 14, section 1 2 and 4) and  
622 orthogonally to it (3 in Fig. 14) they all show that the pre salt Lagoa Feia unit (rift initiation, High and  
623 tectonic changes) has been deposited and controlled by the large listric fault and some of the out of  
624 sequence extensional late fault. As suggested by some reflection termination (Fig. 5d) there is no reason  
625 to rule out the possibility that some of the initial low angle faults may have been in reality part of a pre-  
626 existing inherited structure affecting the Cabiúnas Formation, re activated during the main rifting  
627 activity. Overall the framework seems to suggest a long lived extensional system affected by several  
628 low angle and listric faults which in some cases were re activated during the final subsidence history.  
629 The lateral thickening but also onlapping through an interfingered relationship with the border fault  
630 deposit, suggested that the Lagoa Feia unit is mostly a syn rift depositional unit. In that case they should  
631 not be assigned to the post rift supersequence as originally suggested by Winter et al. (2007). Finally  
632 the faults do not affect the pre salt unit confined between the pre salt syn rift unconformity and the base  
633 salt but there are no obvious relation to rule out the possibility that this unit may still be affected by a  
634 syn rift activity driven by a deep crustal extension devoid of visible upper fault.

635

#### 636 **6.5 Pre-salt post rift unconformity: still tectonically - controlled?**

637 In this paper we restrict the analysis of our observation to specifics single half graben systems located  
638 in the proximal zone of the passive margin (Fig 1) as we do not have data to compare this section with

639 the distal one along the abyssal plane. This pose uncertainty in pushing our interpretation further into  
640 the distal portion of the margin and may explain some clear difference in the depositional system and  
641 tectonic reconstruction proposed by other authors exploring more distal units (Muniz & Bosence, 2018).  
642 We think it is difficult to compare the seismic facies and seismic units observed and proposed in this  
643 paper with the interpreted seismic sections (imaging a more distal part of the Campos basin) discussed  
644 in the paper by Muniz & Bosence (2018) as no details of seismic facies are proposed and most of their  
645 interpretations rely on well log correlation.

646 However using a more regional seismic profile (Line D, 12 sec TWT Fig 15) as reference for the crustal  
647 structure of the area and extending along NW-SE from near the area of our analysis to the more slope  
648 basin part of the margin, we could better define the regional context of our analysis. It is beyond the  
649 scope of this paper to discuss the regional and deep nature of the basement and the regional structure  
650 but we will use this seismic line (Line D) as reference for locating the half graben structure controlling  
651 the Lagoa Feija Group.

652 The seismic line D clearly indicate the top basement (named Top Cabiunas formations, dotted red),  
653 the post rift unconformity (light red bold line) and the base salt units (green bold line) defining  
654 respectively the subunit 4 and the top of the subunit 3. The top basement define below a thick crustal  
655 unit where some clear dipping structure (dotted white colour) plunging ocean-ward can be mapped (also  
656 defined by the base of the parabolic diffractive smiles). The lack of a refraction velocity model doesn't  
657 allow us to define the nature of this discontinuity, but using and comparing the interpretation from a not  
658 far Campos section proposed by Unternehr et al (2010) those features can be interpreted or as a fault or  
659 crust structures affected by a changes of seismic facies. In the shallow part of the seismic line D we  
660 can clearly observe that all the half graben pre salt structures described and interpreted in this paper are  
661 fully located in the proximal continental domain of the Campos basin. The Sub-Unit 4 can be also  
662 clearly interpreted as the pre salt Sag deposition unit draping on top of the syn-rift half graben subunits.  
663 This structural motif is observed all across the area of interest as indicated by interpretation of near  
664 seismic lines (Fig 14).

665 From our mapping (Figs. 5 a to c and Figs. 8-10) but using the interpretation of other near seismic  
666 profile (Fig 14) and a more regional line (Fig 15), the Lagoa Feia Group appear draped by the  
667 transitional late Syn-Rift pre salt sequence (subunit 4) bounded at the base by the pre salt unconformity  
668 (red unit) and at the top by the base salt (green line) and observed at a regional scale (see sections in  
669 Fig 5). It is tectonically characterized by a phase where the differential subsidence across the fault plane  
670 ceases to be important (Figs 5, 8-10) and this is observed all across the proximal area (Fig 14, 15).  
671 Within our area of investigation the surface we interpreted as pre salt unconformity (red line in Figs 5)  
672 separate a domain still affected by faults characterized by lateral thickening unit with coarse grain re  
673 deposited rudstone from a domain where parallel reflector are concordant to the surface and are thinning

674 out versus the inner part of the margin. The two well A and B (Goldberg et al.,2017) indicate this  
675 portion is characterized at the base by the dominance of fine sediments dominated by heterolithics and  
676 massive mudrocks suggesting the action of low-density turbidity currents, associated to distal portions  
677 of turbidite lobes.

678 The seismic lines interpreted (Line A to D) but also the interpretation of near seismic line (Fig 14)  
679 indicate the pre salt unconformity is observed laterally beyond the rift basins (Fig 5a-c) and it  
680 consistently remains below the salt unit (Fig 15). Across the all seismic lines this unit is always a  
681 sedimentary precursor of the salt units characterized by halokinetic features (Fig 5 a to c). Further  
682 insight of the units above the Coqueiros formation, come from the well data description proposed by  
683 Muniz& Bosence (2018), both located in the proximal Badeiro High and External High, in a more distal  
684 portion respect to our dataset but approximately located in the green square indicated in Fig 15. The  
685 authors describe those pre-salt units as characterized by aggradational coarse carbonate grainstones  
686 comprising ooid spherulites and stevensite grain and therefore interpret these units as part of the Macabu  
687 Formation and assign a post rift sag stratigraphic significance.

688 Following the well log correlations, seismic and structural interpretation proposed in this paper and in  
689 the existing literature (Goldberg et al.,2017; Muniz and Bosence, 2018) , the pre salt post-rift unit  
690 assigned to the Macabu Formation may correspond to the onset of a regional lower Aptian  
691 unconformity, termed by some authors (Karner, 2000), as the pre Alagoas unconformity and would  
692 support these units here being interpreted as a gentle sag phase part of the rift supersequence leading to  
693 the evaporitic or salt sequences (Guardado et al.1990; Goldberg et al., 2017).

694 Taking into account a more regional point of view, the lack of upper crustal rift deformation in our  
695 seismic sections (Figs 5 and 8) can't rule out the possibility that this pre salt late-syn rift unit was still  
696 subsiding under the depth-dependent extension determined by the rate of crustal/lithospheric extension  
697 (Karner & Gamboa, 2007). Therefore we cannot exclude that this late syn rift unit could still be related  
698 to the last crustal adjustments or still linked to the deformation transition from fault-controlled brittle  
699 deformation to depth-dependent lithospheric thinning, essentially triggered by ductile stretching of the  
700 lower crust (Kusznir and Karner, 2007). Again the major uncertainty derive from the lack of data  
701 allowing us to trace the relationship of this upper units with the more distal portions of the margin where  
702 the extended crust have been observed (Zalan, 2011). Following the Ocean/continent border unit (Fig  
703 1a) proposed by Zalan (2011), our data appear to be grounded on a proximal high angle fault poorly  
704 extended crust. Nothing really forbid to interpret this succession as a pre salt basin fill, deposited into a  
705 continued late syn-rift extension without major visible extensional faulting typical of the upper crust  
706 (Guardado et al.1990; Karner, 2000; Karner and Gambôa, 2007, Contrera et al., 2010). If so, given the  
707 regional nature of the pre salt post rift unconformity preceding a transgressive unit, that is draping the  
708 main asymmetric graben and preceding the salt deposition the Pre-salt *post-rift unconformity*, that unit

709 can be interpreted as a breakup unconformity followed by a breakup surface (Soares et al., 2012) here  
710 represented by our Unit (4). *Per se* it can merely represent the end of activity in local syn-rift faults,  
711 rather than the true end of crustal stretching and the initiation of the drifting phase on newly formed  
712 divergent margins (Reston, 2005; Péron-Pinvidic et al., 2007, Soares et al., 2012). The lack of regional  
713 seismic line helping us in correlating those structures with the more distal deposition system (potentially  
714 more crustally extended) does not allow us to push further consideration on the regional significance of  
715 our findings.

716

## 717 **7 Conclusion**

718 A seismic and structural interpretation of the pre-salt Lagoa Feia Group is here proposed through the  
719 analysis of a combination of seismic and well data from the Campos Basin. Our analysis shows that:

720- - By using some basic attributes of the seismic signal it is possible to recognize some distinctive seismic  
721 facies characterizing the main lacustrine depositional environment across the entire region of the  
722 Campos Basin.

723- - The main seismic facies, calibrated through well data, can be linked to the main depositional units of  
724 the Lagoa Feia Group, characterizing border fault deposits; dominantly fine-grained re-sedimented  
725 deposits; dominantly coarse-grained, carbonate-rich re-sedimented deposits; and intrusive wipe out  
726 zones affecting the entire pre-salt unit.

727- - The seismic facies allow the description and characterization of an internal seismic architecture of the  
728 sub-basin related to the syn-rift tectonic activity, suggesting that the Lagoa Feia seismostratigraphy  
729 represents a fault-restricted lacustrine depositional environment, strongly affected by long-lived  
730 intermittent rift tectonics.

731- - Restoration models suggest that the extensional rift tectonics has been intermittent but affected by  
732 different populations of normal faults through the pre salt depositional history. All the faults likely  
733 contributed to trigger the main re depositional nature of the main lacustrine deposit but also to shape  
734 the syncline geometry of the main half graben preserving the Lagoa Feia unit.

735- - The Unit embedded between the pre-salt late-rift unconformity and the base salt unit, is draping the  
736 all half graben faults controlled. It is un-affected by faults and the well correlation (Goldberg et al.,2017;  
737 Muniz & Bosence, 2018) suggest it can be interpreted as stratigraphically equivalent to the Macabu  
738 Formation. The pre-salt late-rift unconformity may represent a breakup unconformity followed by an  
739 intermediate (syn- rift) sag phase preluding to the salt deposit affecting the entire Campos basin.

740

741 **Acknowledgement:** The authors thank BG Brasil, a wholly owned subsidiary of Royal Dutch Shell  
742 plc, for financial support for this project and permission to publish. This work was sponsored by the  
743 BG funded Deep Rift project (BG-UFRGS-Aberdeen). The paper used Petrel (Schlumberger) and  
744 Geoteric (ffA) to interpret the seismic dataset. Constructive comments on an initial draft by T.Alves  
745 and Moriak , Douglas Paton are greatly appreciated. We thanks Brent Wignall for comments.

746

## 747 **Bibliography**

748

749 Abrahao, D., Warme, J.E. 1990. Lacustrine and associated deposits in a rifted continental margin-lower  
750 Cretaceous Lagoa Feia Formation, Campos Basin, Offshore Brazil. in Lacustrine Basin Exploration,  
751 Case Studies and Modern Analogs, Vol. 50, pp. 287–305, ed. Katz B.J., AAPG Memoir.

752

753 Amaral, G., Cordani, U. G., Kawashita, K., and Reynolds, J. H, 1966.Potassium argon dates of basaltic  
754 rocks from southern Brazil. *Geochim. Cosmochim. Acta*, 30:159-189.

755

756 Alvarenga, R., Iacopini, D., Kuchle, J., Scherer, C. & Goldberg, K. 2016. 'Seismic characteristics and  
757 distribution of hydrothermal vent complexes in the Cretaceous Offshore Rift Section of the Campos  
758 Basin, Offshore Brazil'. *Marine and Petroleum Geology*.

759

760 Armelenti, G.,Goldberg, K., Kuchle, J., De Ros. L.F. 2016 Deposition, diagenesis and reservoir  
761 potential of non-carbonate sedimentary rocks from the rift section of Campos Basin, Brazil. *Pet.*  
762 *Geosci.*, 22, 223-239

763

764 Brown, L.F., Fisher, W.L., 1977. Seismic-stratigraphic interpretation of depositional systems: examples  
765 from Brazilian rift and pull-apart basins. In: PAYTON, C.E. (Ed.) *Seismic stratigraphy: applications to*  
766 *hydrocarbon exploration*. AAPG, Memoir 26, Tulsa, p. 213-248.

767

768 Chopra, S., Marfurt, K.J. 2007. Seismic attributes for prospect identification and reservoir  
769 characterization. SEG books.

770

771 Chopra S, Castagna J P., Xu Y. Relative acoustic impedance defines thin reservoir horizons. *Search and*  
772 *Discovery Article #40435 (2009)*

773

774 Contrera, J., Zuhlke., Bowman., S., Bechstadt., T., (2010). Seismic stratigraphy and subsidence  
775 analysis of the southern Brazilian margin (Campos, Santos and Pelotas basins). *Marine and Petroleum*  
776 *Geology*. 27, 1952-1980.

777

778 Demercian S., Szatmari P., Cobbold P.R. 1993. Style and pattern of salt diapirs due to thin-skinned  
779 gravitational gliding, Campos and Santos basins, offshore Brazil. *Tectonophysics*, 228, 393-433

780

781 Colpaert,A., Pickard,N., J Mienert, j., Henriksen,L.B., Rafaelsen, b., Andreassen, K.. 2007 3D  
782 seismic analysis of an Upper Palaeozoic Carbonate succession of the Eastern Finnmark Platform area  
783 Norwegian Barents Sea. *Sedimentary Geology*, 79-98.

784

785 Davison. 1999. Tectonics and hydrocarbon distribution along the Brazilian South Atlantic margin. In:  
786 Cameron, N. R., Bate, R. H. & Clure, V. S. (eds) *The Oil and Gas Habitats of the South Atlantic*.  
787 Geological Society, London, Special Publications, 153, 133-151

788

789 Davison, I. 2007. Geology and tectonics of the South Atlantic Brazilian salt basins. In: Reis, A. C.,  
790 Butler, R. W. H. & Graham, R. H. (eds) *Deformation of the Continental Crust: the Legacy of Mike*  
791 *Coward*. Geological Society, London, Special Publications, 272, 345–359.

792

793 Dahlstrom, C.D.A., 1969. Balanced cross sections. *Canadian Journal of Earth Sciences*, 6(4), pp.743-  
794 757.

795

796 De Matos. M; Osorio P., Johann, PRS. 2007. Unsupervised seismic facies analysis using wavelet  
797 transform and self-organizing maps. *Geophysics*, 72, 9-22.

798

799 Duda, R.O.,Hart, P. O., and Stork, D.G. 2001, *Pattern classification*, 2nd ed.:JohnWiley & Sons, Inc.

800

801 Gibbs, A.D., 1983. Balanced cross-section construction from seismic sections in areas of extensional  
802 tectonics. *Journal of structural geology*, 5(2), pp.153-160.

803

804 Gibbs, A.D., 1984. Structural evolution of extensional basin margins. *Journal of the Geological Society*,  
805 141(4), pp.609-620.

806

807 Goldberg, K., Kuchle, J., Scherer, S; Alvarenga, R. Ene, PL., Armelenti. G. 2017. Re-sedimented  
808 deposits in the rift section of the Campos Basin. *Marine and Petroleum Geology* 80, 412-431

809

810 Haralick, R. M., K. Shanmugam, and I. Dinstein, 1973, Textural features for image classification: *IEEE*  
811 *Transactions on Systems, Man and Cybernetics*, SMC-3, 610–621.

812

813 Hart, B.S (2008) Channel detection in 3D seismic data using sweetness, *AAPG*, 92, 733-742.

814

815 Herlinger, EJ; Zambonato, EE., De Ros L.F. (2017) Influence of the diagenesis on the quality of the  
816 lower cretaceous pre salt lacustrine carbonate reservoir from northern Campos Basin, Offshore Brazil,  
817 *Journal of Sedimentary Research*, 87, 1285-1313.

818

819 Karner, G.D. (2000) Rifts of the Campos and Santos Basins, Southeastern Brazil: Distribution and  
820 Timing, *AAPG Memoir* 73, 301-315.

821

822 Karner, G. D. & Gamboa, L. A. P. 2007. Timing and origin of the South Atlantic pre-salt sag basins  
823 and their capping evaporates. In: Schreiber, B. C., Lugli, S. & Babel, M. (eds) *Evaporites through Space*  
824 *and Time*. Geological Society, London, Special Publications, 285, 15–35.

825

826 Kumar, N., L. A. P. Gamboa, B. C. Schreiber, and J. Mascle (1977), Geologic history and origin of Sao  
827 Paulo Plateau (southeastern Brazilian margin), comparison with the Angolan margin, and the early  
828 evolution of the northern South Atlantic, in *Initial Reports of the Deep Sea Drilling Project*, vol. 39,  
829 edited by P. R. Supko and K. Perch-Nielsen, pp. 927–945, Texas A & M Univ., College Station, Tex.

830

831 Magee, C., Maharaj, S.M., Wrona, T., and Jackson, C.A.L., 2015, Controls on the expression of  
832 igneous intrusions in seismic reflection data: *Geosphere*, v. 11, p. 1024–1041, doi: 10.1130/  
833 /GES01150.1

834

835 Mohriak, W., Szatmari, P. & Anjos, S. M. C. (eds) 2008. Salt: Geologia e Tectonica. Beca Edicoes  
836 Ltda, Sao Paulo, Brazil.

837

838 Mitchum Jr., R.M., Vail, P.R., Sangree, J. B., 1977. Seismic stratigraphy and global changes of sea  
839 level, Part 6: Stratigraphic interpretation of seismic reflection patterns in depositional sequences. In:  
840 Payton, C.E. (ed.). Seismic Stratigraphy - Applications to Hydrocarbon Exploration. Tulsa, AAPG, 117-  
841 133 (Memoir # 26).

842 Mizusaki, A.M.P., Thomaz Filho, A. Valença, J.G. 1988. VolcanoSedimentary Sequence of Neocomian  
843 age in Campos Basin (Brazil). Revista Brasileira de Geociências, 18:247-251.

844

845 Mohriak. W.U., Mello, M.R., Dewey, J.F., Maxwell., J.R, 1990. Petroleum geology of the  
846 Campos Basin, offshore Brazil. Geological Society London Special Publications 50(1):119-  
847 141

848 Mohriak, W. U., Hobbs, r. & Dewey, J. F. . 1990. Basin-forming processes and the deep structure of the  
849 Campos Basin, offshore Brazil. Marine and Petroleum Geology, 7, 94–122.

850

851 Moriak, W U, Szatamri,P. Anjos, S. 2012. Salt: geology and tectonics of selected Brazilian basins in  
852 their global context. From:Alsop, G. I.,Archer, S. G.,Hartley, A. J.,Grant, N. T.&Hodgkinson, R. (eds)  
853 2012. Salt Tectonics, Sediments and Prospectivity. Geological Society, London, Special Publications,  
854 363, 131–158.

855

856 Muniz, M.C, Bosence, D.W.J. 2018. Lacustrine carbonate platforms; facies, cycles and tectono-  
857 sedimentary models for the pre-salt Lagoa Feia Group (Early Cretaceous), Campos Basin, Brazil.  
858 AAPG Bulletin, in press. doi: 10.1306/051118162061708

859 Mohriak,W.U.,Nemčok., N and Enciso.,G. 2008. South Atlantic divergent margin evolution: rift-border  
860 uplift and salt tectonics in the basins of SE Brazil. Geological Society, London, Special Publications  
861 2008, v. 294, p. 365-398

862 Moulin, M., D. Aslanian, M. Rabineau, M. Patriat, and L. Matias (2012), Kinematic keys of the Santos-  
863 Namibe basins, in Conjugate Divergent Margins, Spec. Publ., vol. 369, edited by W. U. Mohriak et al.,  
864 Geol. Soc., London.

865 Peron-Pinvidic, G., Manatschal, G., Minshull, T.A., Sawyer, D.S., 2007. Tectonose-  
866 dimentary evolution of the deep Iberia–Newfoundland margins: evidence for a  
867 complex breakup history. *Tectonics* 26, TC2011.  
868

869 Posamentier, H., Kolla, V, Seismic Geomorphology and Stratigraphy of Depositional Elements in  
870 Deep-Water Settings 2003, *Journal of Sedimentary Research*, 73, 367–388.  
871

872 Prosser, S. Rift related linked depositional system and their seismic expression. 1993 From Williams  
873 G.D & A.Dobb, 1993. *Tectonics and seismic sequence stratigraphy. Geological Society Special*  
874 *Publication*, 71, 35-66.  
875

876 Prather, B. E., J. R. Booth, G. S. Steffens, and P. A. Craig, 1998, Classification, lithologic  
877 calibration, and stratigraphic succession of seismic facies of intraslope basins, deep-water Gulf of  
878 Mexico; errata: AAPG bulletin, v. 82, p. 707R  
879

880 Prather B. E., Booth J. R., Steffens G. S, and Craig P. A.. 1998. Classification, Lithologic Calibration,  
881 and Stratigraphic Succession of Seismic Facies of Intraslope Basins, Deep-Water Gulf of Mexico.  
882 AAPG Bulletin, 82, 701–728.  
883

884 Radovich, B. J., and R. B. Oliveros, 1998, 3-D sequence interpretation of seismic instantaneous  
885 attributes from the Gorgon field: *The Leading Edge*, 17, 1286–1293.  
886

887 Rangel, H.D., Martins, F.A.L., Esteves, F.R., Feijó, F.J. 1994. Bacia de Campos. *Boletim de*  
888 *Geociências da PETROBRAS*, 8:203-218.  
889

890 Reed IV, T.B. and Hussong, D. 1989. Digital image processing techniques for enhancement and  
891 classification of SeaMARC II Side Scan Sonar Imagery. *Journal of Geophysical Research* 94: doi:  
892 10.1029/89JB00409. issn: 0148-0227.  
893

894 Reston, T.J.,2005. Polyphase faulting during the development of the west Galicia rifted margin. Earth  
895 Planet. Sci. Lett. 237, 561–576.

896

897 Sarg J. F., James S. Schuelke. 2003. Integrated seismic analysis of carbonate reservoirs: From the  
898 framework to the volume attributes *The Leading Edge*, 2, 640-645

899

900 Soares ,DM., Alves M.T, Terrinha, P. 2012. The breakup sequence and associated lithospheric breakup  
901 surface: Their significance in the context of rifted continental margins (West Iberia and Newfoundland  
902 margins, North Atlantic) . *Earth Planetary Sciecn Letters*, 355, 311-336.

903

904 Stanton N., Masini, E. 2013.The rifting evolution of the Santos Basin: A Geophysical view. 13th  
905 International Congress of the Brazilian Geophysical Society & EXPOGEF, Rio de Janeiro, Brazil, 26–  
906 29 August 2013: pp. 1690-1693. [doi.org/10.1190/sbgf2013-346](https://doi.org/10.1190/sbgf2013-346))

907

908 Taner, M. T., and Sheriff, R. E., 1977, Application of amplitude, frequency,and other attributes to  
909 stratigraphic and hydrocarbon determination,in Payton, C. E., Ed., *Seismic stratigraphy—applicationsto*  
910 *hydrocarbon exploration: AAPG Memoir*, 26, 301–327.

911

912 Taner,M. T., Schuelke, J. S., O’Doherty, R., and Baysal, E., 1994, Seismic attributes revisited: 64th  
913 *Ann. Internat. Mtg., Soc. Expl. Geophys.,Expanded Abstracts*, 1104–1106

914

915 Tedeschi et al., 2017. New age constraints on Aptian evaporites and carbonates from the South  
916 Atlantic: Implications for Oceanic Anoxic Event 1a: *Geology*, doi:10.1130/G38886.1.

917

918 Vail, P.R., Todd, R.G. & Sangree, J.B., 1977. Seismic Stratigraphy and Global Changes of Sea Level,  
919 Part 5: Chronostratigraphy Significance of Seismic Refletions. In: Payton, C. E. (ed.). *Seismic*  
920 *Stratigraphy – Applications to Hydrocarbon Exploration. Tulsa, AAPG Memoir 26*, p. 99-116.

921

922 Vinther, R., K. Mosegaard, K. Kierkegaard, I. Abatzis, C. Andersen, O. Vejbaek, F. If, and P. Nielsen,  
923 1995, Seismic texture classification: A computer-aided approach to stratigraphic analysis: 65th Annual  
924 International Meeting, Society of Exploration Geophysicists Expanded Abstracts, v. 95, p. 153–155.

925 Wright, V.P., 2012, Lacustrine carbonates in rift settings: the interaction of volcanic and microbial  
926 processes on carbonate deposition, in Garland, J., Neilson, J.E., Laubach, S., and Whidden, K.J., eds.,  
927 Advances in Carbonate Exploration and Reservoir Analysis: Geological Society of London, Special  
928 Publication 370, p. 39–47.

929 Wright, V.P., and Barnett, A.J., 2015. An abiotic model for the development of textures in some South  
930 Atlantic Early Cretaceous lacustrine carbonates, in Grotzinger, J.P., and James, N., eds., Microbial  
931 Carbonates in Space and Time: Implications for Global Exploration and Production: The Geological  
932 Society of London, Special Publication 418, p. 209–219.

933

934 Zalán, P. V., M. d. C. G. Severino, C. A. Rigoti, L. P. Magnavita, J. A. B. De Oliveira, and A. R. Vianna  
935 2011, An entirely new 3D-view of the crustal and mantle structure of a South Atlantic Passive Margin—  
936 Santos, Campos and Espírito Santo Basins, Brazil, in AAPG Annual Convention and Exhibition,  
937 Houston, Texas.

938

939 Weszka, J., Dyer, C., Rosenfeld, A., 1976. A comparative study of texture measures for terrain  
940 classification. IEEE Trans.Systems Man Cybernet. 6, 269–285.

941

942 Winter, W. R.; Jahnert, R. J.; França, A. B. 2007. Bacia de Campos. Boletim de Geociências da  
943 Petrobras, Rio de Janeiro. v. 15, n. 2, p. 511-529.

944

945 Zhang, Z., and M. Simaan, 1989, Knowledge-based reasoning in SEISIS: A rules-based system for  
946 interpretation of seismic sections based on texture, in F. Aminzadeh and M. Simaan, eds., Expert  
947 systems in exploration: Society of Exploration Geophysicists Geophysical Development Series, v. 3, p.  
948 141–159.

949

950 **Figure captions:**

951 Figure 1: a) Location of the study area offshore Campos Basin, southeastern Brazil. COB  
952 (Continental Ocena Boundary following Zalan et al.,2011); b) Seismic grid of the 2D lines

953 analyzed for this studies. In bold the location of the three seismic lines (L.A, L.B and L.C)  
954 selected and the two well data (A and B) which were utilized for this studies.

955 Figure 2 : Schematic table representing : the main lithostratigraphic units, seismic stratigraphy  
956 units recognized and proposed in this study, the main regional tectonic framework and the  
957 super-sequences (sensu Winter et al., 2001) for comparison. The color within the seismic  
958 stratigraphy units represents the mapped horizons and unconformities as represented in the  
959 interpreted seismic line..

960 Figure 3. a) seismic image indicating a Red Green and Blue (RGB) blended image using  
961 three main frequencies (15 Hz red, 35 Hz green, 55 Hz Blue Hertz). In white are represented  
962 the areas with a concentration of the three frequencies. The arrow points respectively the top  
963 and the bottom of the salt unit and the main rudstone-coquinas units. (b) Representation of  
964 part of the Well B calibrating some of the reflectors within the sub-salt Lagoa Feia. The white  
965 points represents the interval velocity from check shot data (2519m/sec; 2402 m/sec). The  
966 thickness of a single reflection is also represented. The colors legend represent the principal  
967 lithological information observed from well core data released. (c) the diagram show the  
968 velocity function obtained from the check shots. The average velocity obtained from the  
969 diagram are represented with bold brown and blue line along the well. White numbers  
970 represents the depth position.

971 Figure 4 Synthetic overview of the various attributes applied (Cosine of the phase; RMS  
972 amplitude; Relative Acoustic Impedance) and a description of their utility and interpretation  
973 rules within our seismic facies analysis is represented.

974 . Figure 5: All lines are TWT time seismic line represented as 3x vertical exaggeration. The  
975 depth scale has been calculated using the velocities scheme proposed in figure 3C. A).  
976 Seismic line A represented as amplitude expression with 3x vertical exaggeration. White  
977 lines represent the main rift faults. Red numbers 1, 2 and 3 represent respectively the three  
978 main faults family recognized: 1. late syn-rift west dipping fault; 2. Syn-rift east dipping  
979 faults. 3. Syn rift pseudo listric fault. Mapped horizons from youngest to oldest: red the post  
980 rift unconformity; blue the maximum rifting surface; dotted orange the half graben  
981 development surface; dotted red the Top cabiunas formation; the yellow sub section (boxes)  
982 focus on the reflection termination toward the faults. They are magnified below the main  
983 seismic section with the white arrows pointing at the reflection terminations geometry. The

984 white numbers (1,2 and 3) as pointed by the white arrows across the all image 5a to c  
985 represents areas characterized by distinctive reflection terminations respect to the main syn-  
986 rift fault system . Sub section1 show the onlap geometry of the syn rift deposit; Sub section 2  
987 show the reflectors (relatively bright) cutted off by the faults. B). Seismic line B and the main  
988 Well B representing the main lithological units;. Subsection 1) Reflectors on-lapping on the  
989 west dipping syn rift fault. Subsection 2) Lateral thickening reflectors but on-lapping on a  
990 chaotic zone bordering the syn-rift fault. Subsection 3) reflector on-lapping on the main fault  
991 but concordant respect to the top Cabiunas formation; C). Seismic line A crossed by the well  
992 A and well C. Sub section1 show the onlap geometry of the syn rift deposit; Sub section 2  
993 show the reflectors (relatively bright) cutted off by the faults.

994 Figure 6. Representation, imaging and description of the main seismic facies (1 to 4)  
995 observed and recognized in the sub- salt Campos Basin.

996 Figure 7 a, b . Seismic attributes images extracted and zoomed from the seismic line A  
997 represented in figure 5 A. A) seismic image represented as relative acoustic impedance. Note  
998 the clear and distinctive seismic facies 2 and 3 defined by the different brightness and (dis-  
999 )continuity. B) seismic reflectors from (a) now expressed as cosine of the phase. Note the  
1000 facies 2, 3 are now characterized by distinctive thickness and (dis-)continuity properties.

1001 Figure 8. Seismic line C (4x vertically exaggerated) and crossed by the well A, showing the  
1002 distribution of the main seismic facies 1,2 and 3. Numbers 1, 2 and 3 represent the units  
1003 characterized by the proposed facies 1, 2 and 3 (see main text). The dotted lines represent the  
1004 boundaries between the main seismic facies.

1005 Figure 9. Seismic line A with the location of the well B and the mapped seismic facies (1-3).  
1006 Numbers 1, 2 and 3 represent the units characterized by the proposed facies 1, 2 and 3 (see  
1007 main text). The dotted lines represent the boundaries between the main seismic facies.

1008 Figure 10 Seismic line A with the location of the well B and the mapped seismic facies (1-3).  
1009 Numbers 1, 2 and 3 represent the units characterized by the proposed facies 1, 2 and 3 (see  
1010 main text). The dotted lines represent the boundaries between the main seismic facies.

1011

1012 Figure 11. Enlarged view of the seismic line A (from figure 10) with the location of the well  
1013 B. In orange are represented the conglomerate and arenitic sandstones; in blue and  
1014 aquamarine the coarse grained/rudstone carbonate/coquinas units; in pale green silty  
1015 argillite; strong green the shale and grey the marly units. The basalts in the Cabiúnas  
1016 Formation are marked with the purple colour.

1017 Figure 12 Representation of the main facies across the pre salt units; Seismic line A. In  
1018 orange is represented the seismic facies 1; In green the seismic facies 2; In blu the seismic  
1019 facies 3.

1020 Figure 13 Kinematic restoration test of Line A. a) Mapped normal faults and main units of  
1021 the pre-salt interval, corresponding to described systems tracts and seismic facies referred to  
1022 in the text. B) Pre-rifting geometries with dashed fault locations. C) Scenario 1, in which  
1023 Fault set 2 pre –dates Fault 3 and depositional geometries of the lower part of the lagoa Feia  
1024 Fm are largely controlled by Fault Set. d) Scenario 2: kinematically linked fault sets, in which  
1025 Fault set 2 branches off a detachment floor fault, which may be linked to Fault 3. e) Border  
1026 fault 3 zone formation, with Seismic Facies q related to slump deposits and possible hanging-  
1027 wall collapse. f) Activation of Fault Set 1, which post-dates movement on other fault  
1028 populations and the deposition of the Lagoa Feia Fm.

1029 Figure 14: Schematic sections of the major sub basin structures mapped in the Campos Basin  
1030 . A) the large scale normal fault/rift related structures as mapped from the seismic dataset. In  
1031 green the trace representing the main sections shown in B. B) Some examples of the rift  
1032 structures and their syn/post rift units mapped and interpreted in this work. In yellow the rift  
1033 initiation system track, blue: high tectonic activity system track; purple: low tectonic activity  
1034 systems tract. Green: the SAG/salt units.; pale blue: passive margin units; white: sea water.

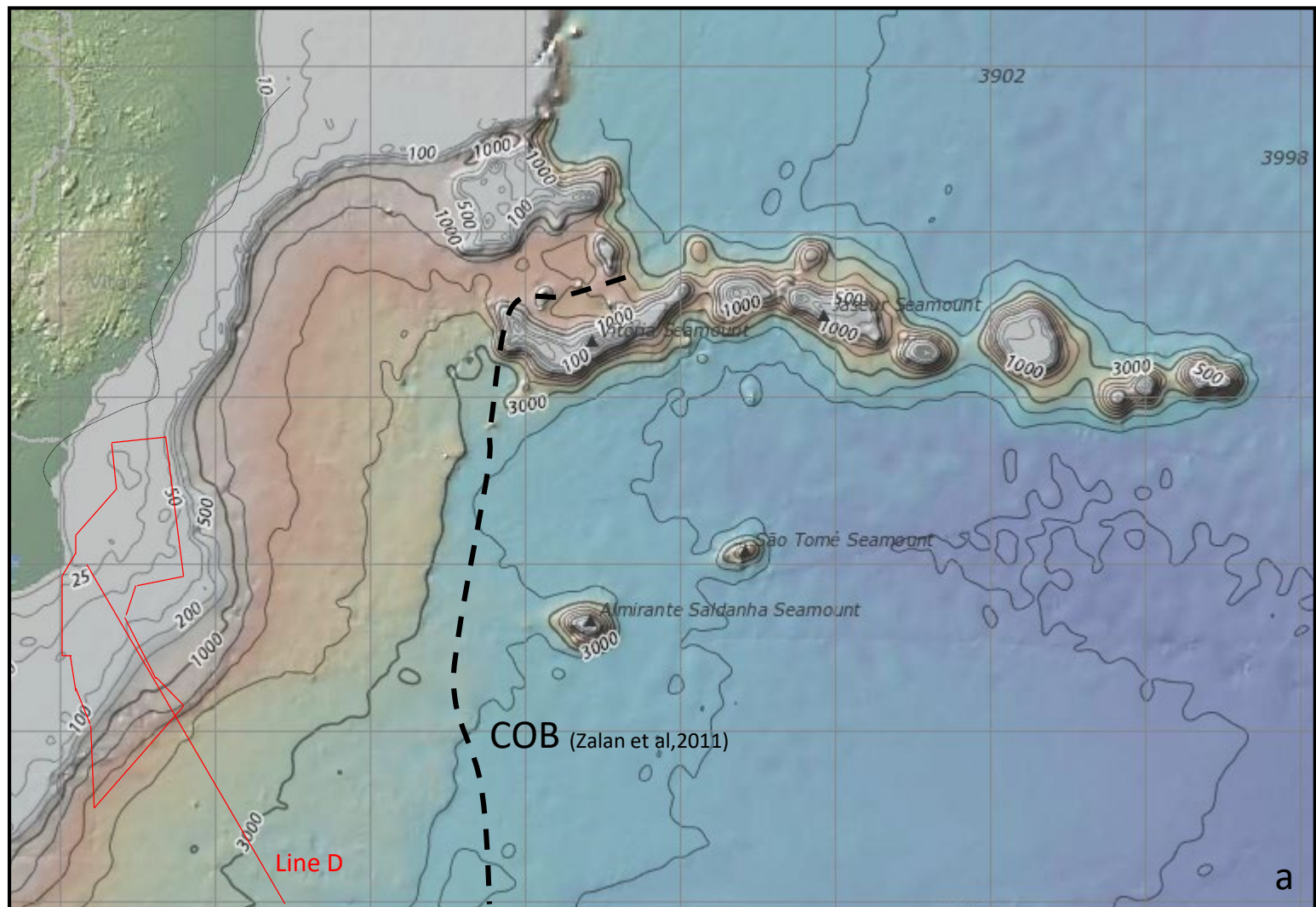
1035 Fig 15. This represent a regional seismic lines (Line D, courtesy of BG) with indicated the  
1036 main regional units. In dotted red: Top Cabiunas formation; Bold red: Post rift Unconformity;  
1037 Bold green: the base and top unit of the Salt. In bold Blue the the Neogene base. The yellow  
1038 box in the proximal zones, represent the location of the intepeted Lines from A to C. In  
1039 dotted green is represented the equivalent location of the Lines interpreted by Muniz &  
1040 Bosence 2018.

1041

1042

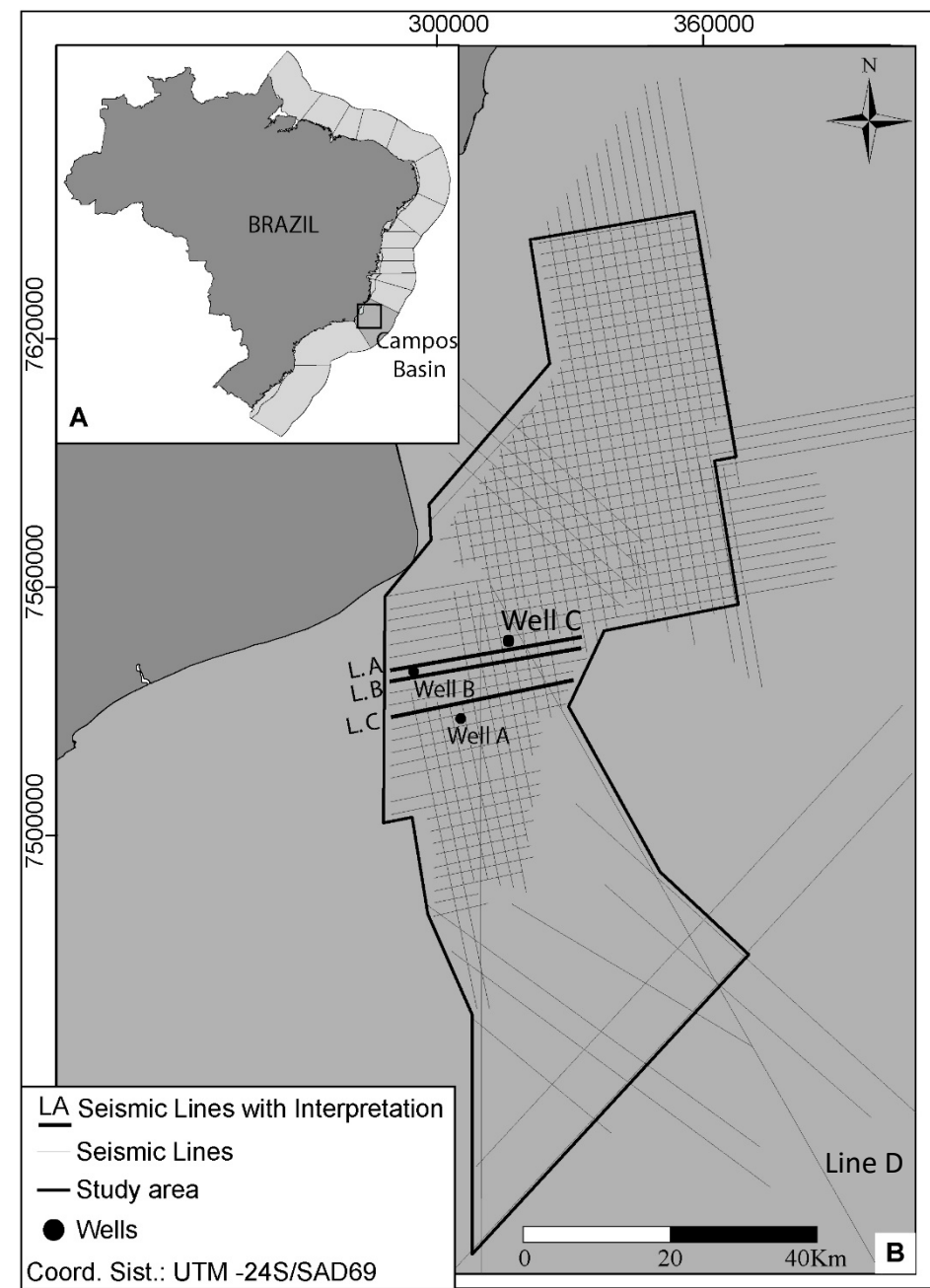
1043

1044



42W

33W



Litho-stratigraphy	Age Ma	Stratigraphic Framework This Paper	Rifting Process This paper	Super Sequence (Winter et al., 2001)
Sea		Sea <span style="float: right;">Sea bottom</span>		
Campos/ Macaé Form		Passive Margin	Post - Rift	Drift
Retiro Fm. Salt	113	Salt base		
L a g o a  F e l i a  G R	118/ 124	<b>SAG?</b>  Pre salt- post rift unconformity Surface?		Post-rift ??
		Late Rift climax system Tract		↑
	Undef?	Tectonic change Surface		↓
Itabapoana Form (Coqueiros Form Equivalent)		High Tectonic Activity System Tract	Syn-Rift	Rift
Atafona Form		Half graben development surface		
Cabiunas Fm	130	Rift Initiation System Tract  Cabiunas top		
	135/ 540	Pre-rift unconformity		↓
Basement		PRE-RIFT	Pre-Rift	

Fig 2

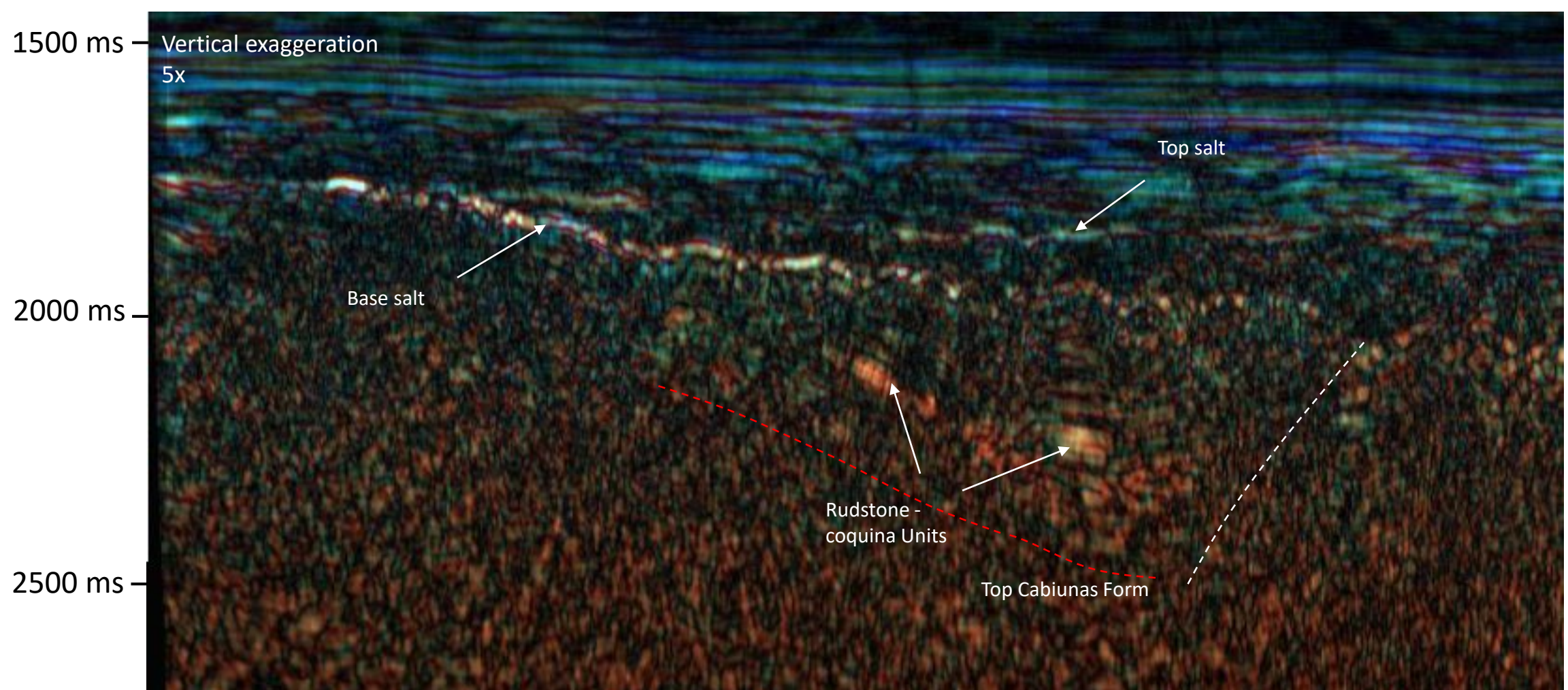


Fig 3A

### Well B

### Legend

- |   |   |
|---|---|
|  Silty-argillite                 |  Calcilutite |
|  Conglomerate                    |  Calcarenite |
|  Shale                           |  Coquina     |
|  Arenite                         |  Gypsum/Salt |
|  Basalt/diabase<br>Cabiunas Form |  Marl        |

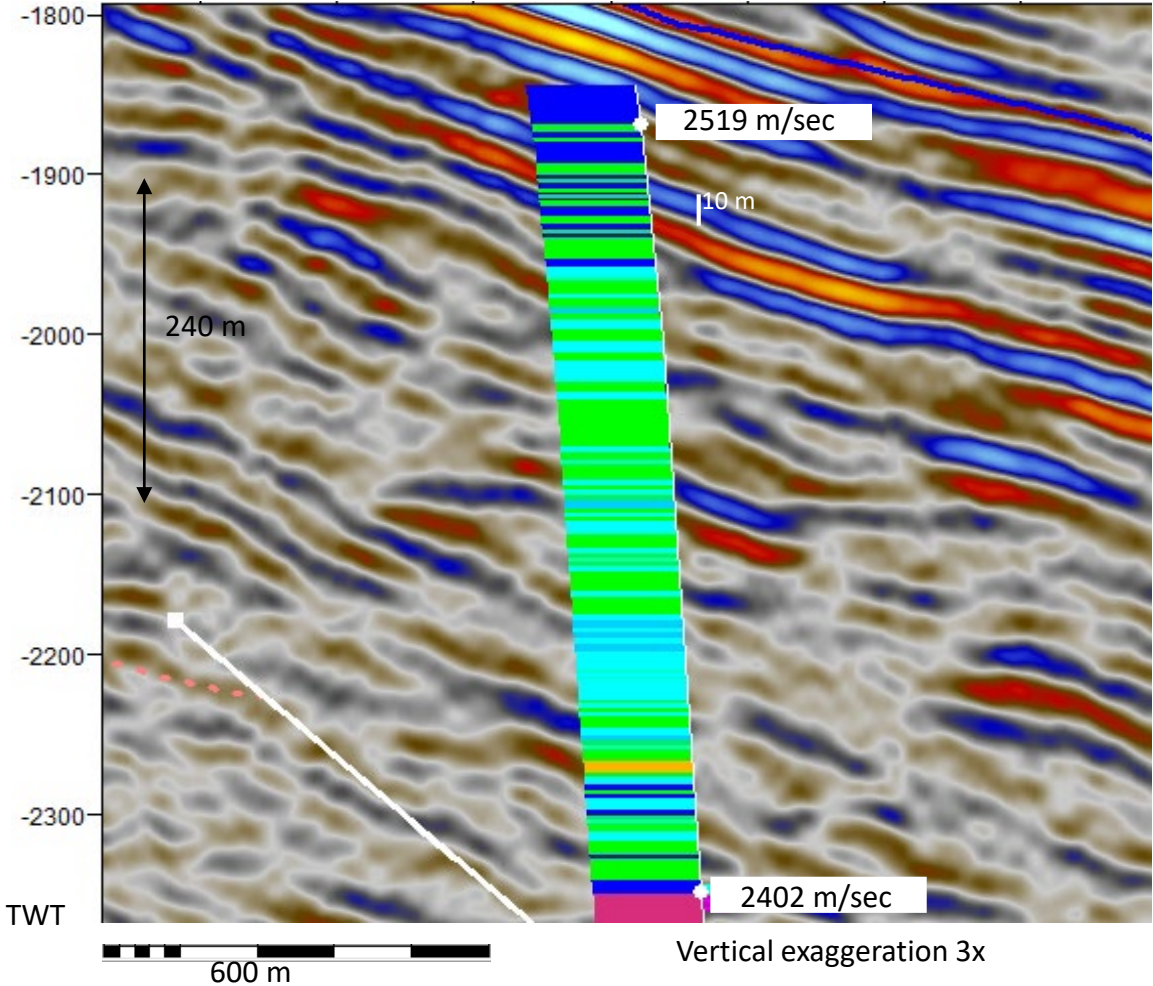


Fig 3B

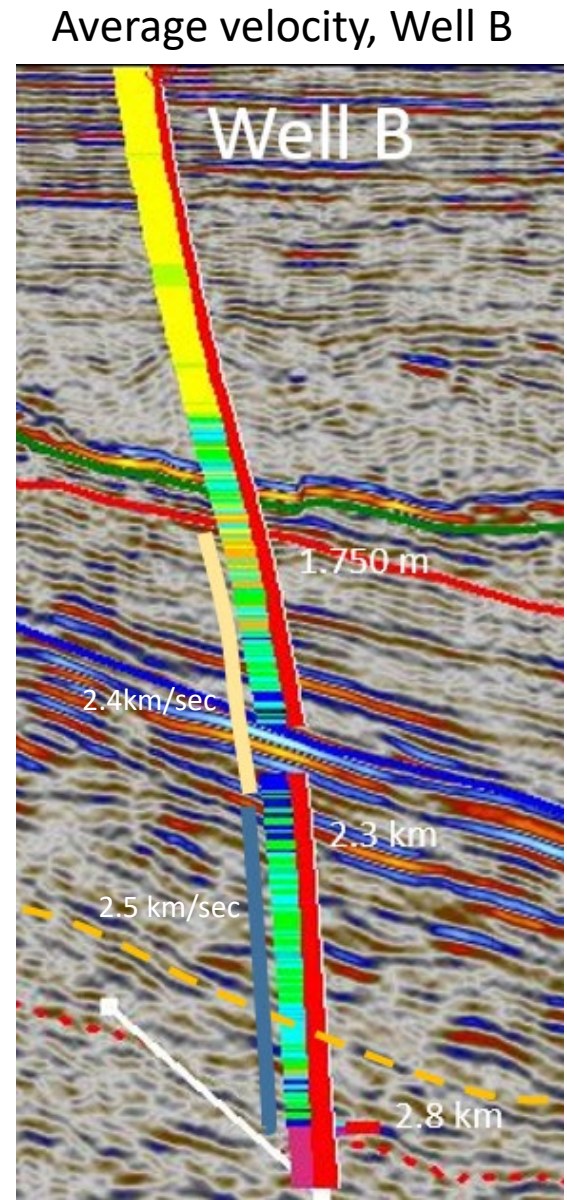
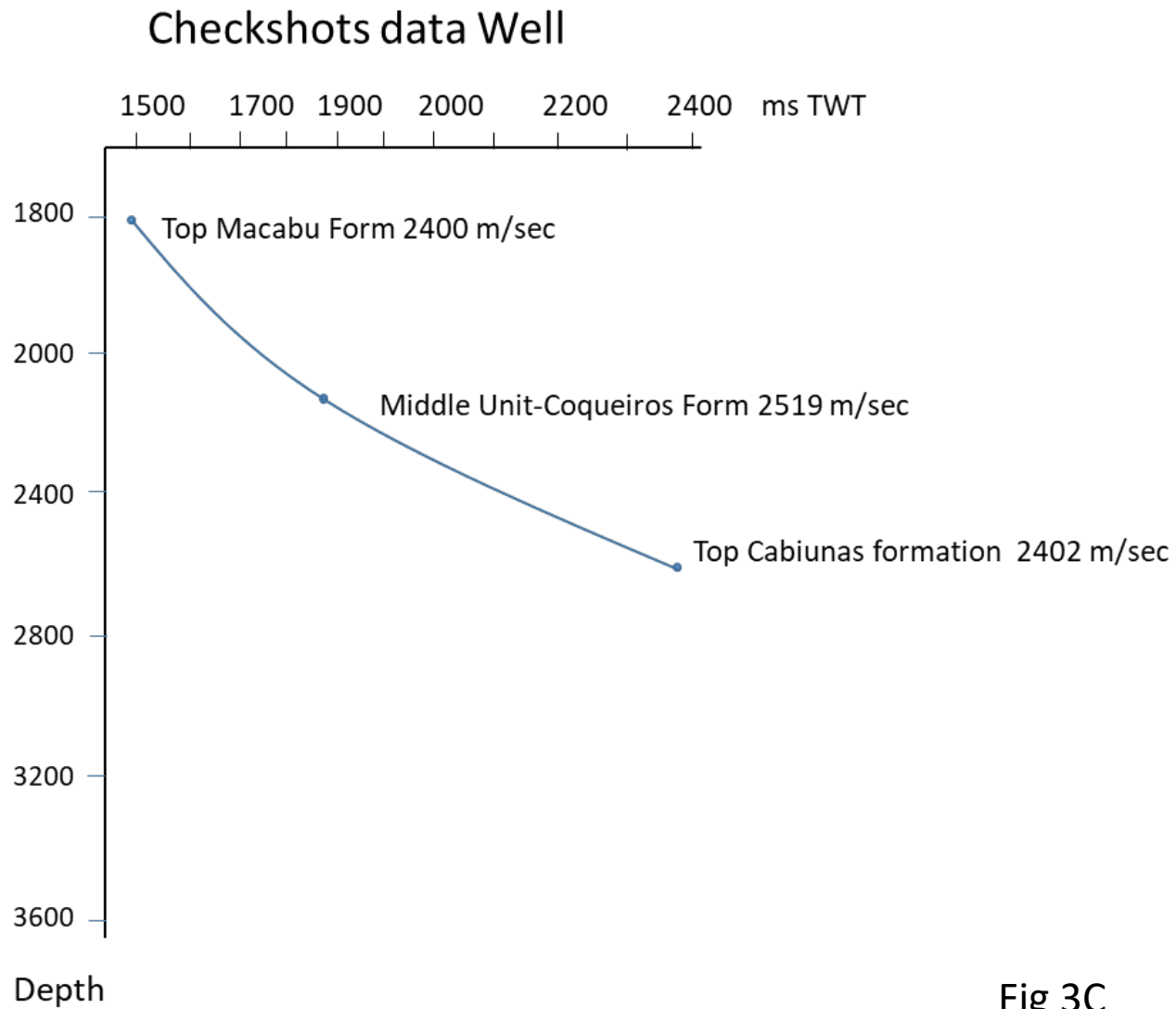


Fig 3C

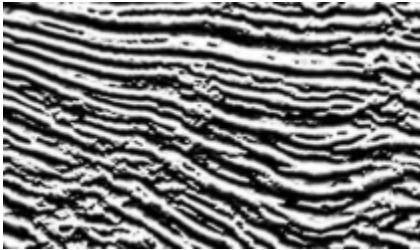
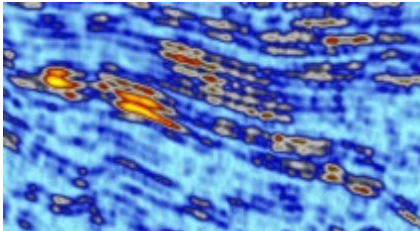
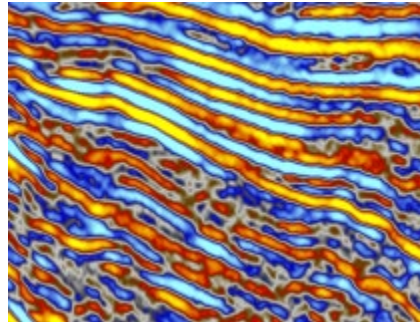
Seismic attributes	Utilities for the paper	Interpretation rules	Visual expression
Cosine Phase	Check Continuity of reflection patterns ; enhance fault visualization	Use the boundaries between patterns	
RMS Amplitude	Enhance seismic facies -mainly for carbonates and evaporites- -Good to map the base of salt	Makes Peak & Trough as (+)	
RAI – Relative Acoustic Impedance	Enhances seismic facies -mainly carbonates and evaporites -good to map base of salt -together with cosine phase, to map faults	Inversion of Peak & Trough P – (-); T – (+) - Enlarge the reflection frequency - Highlight the signal texture	

Fig 4

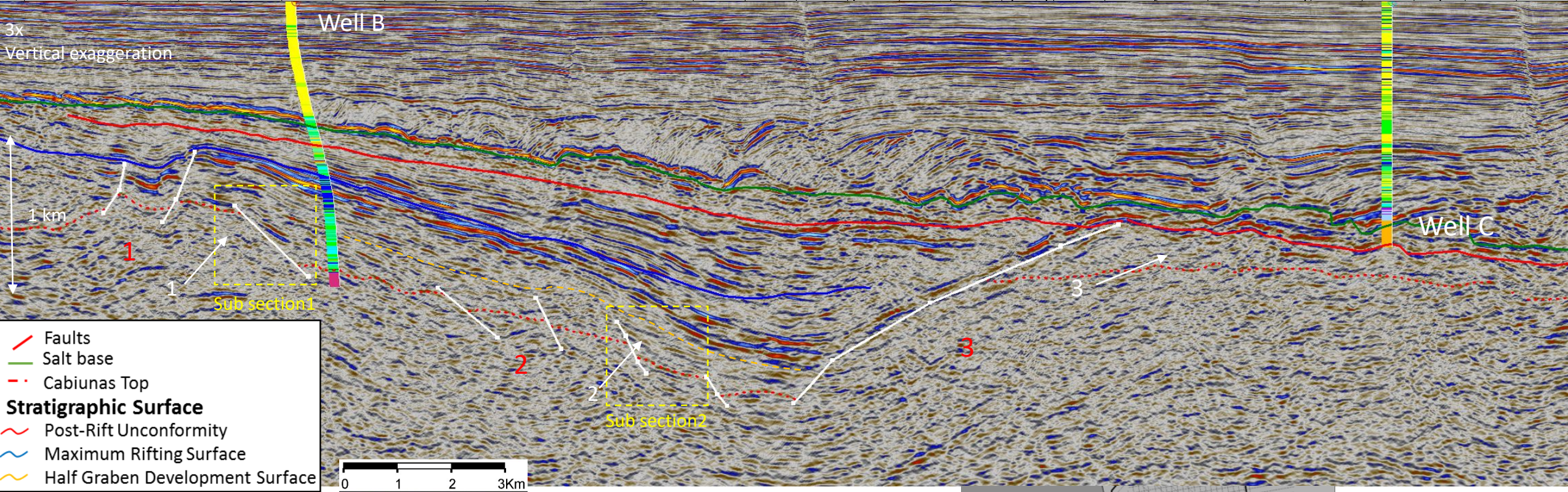
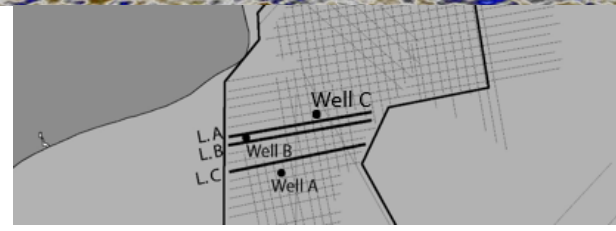
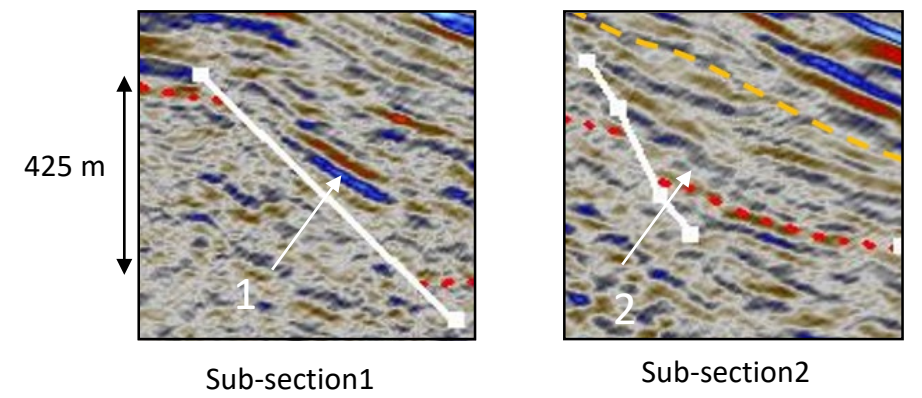


Fig 5A



Seismic Line A

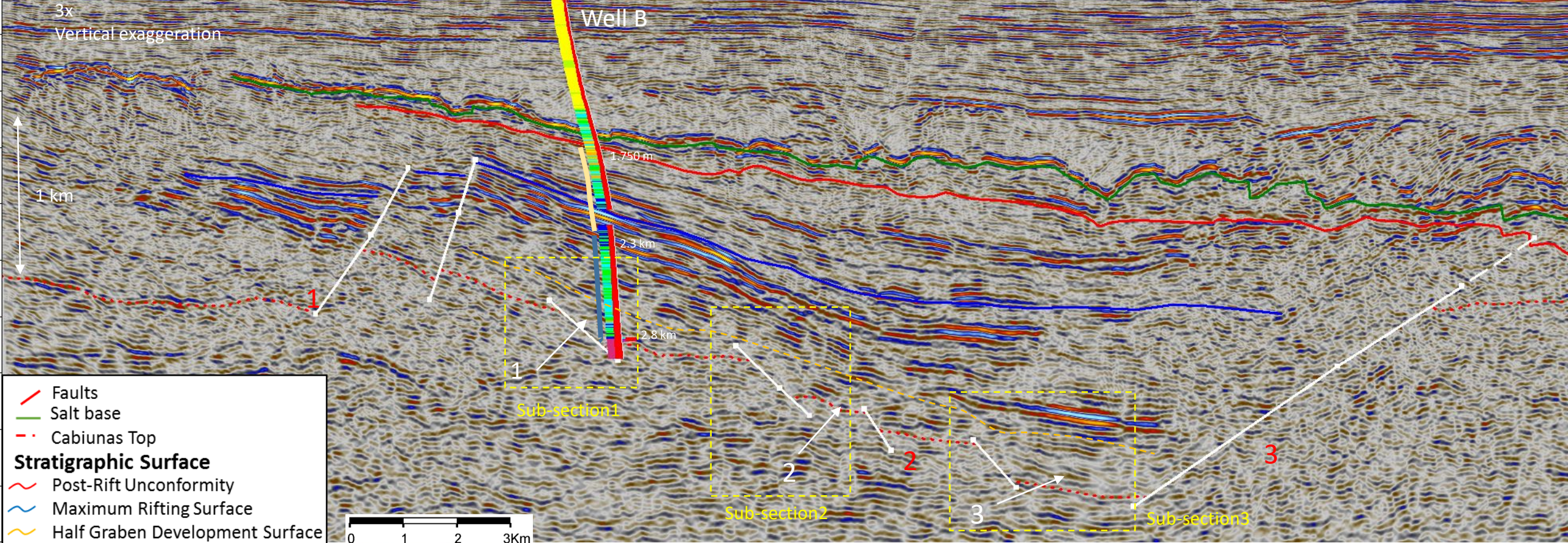
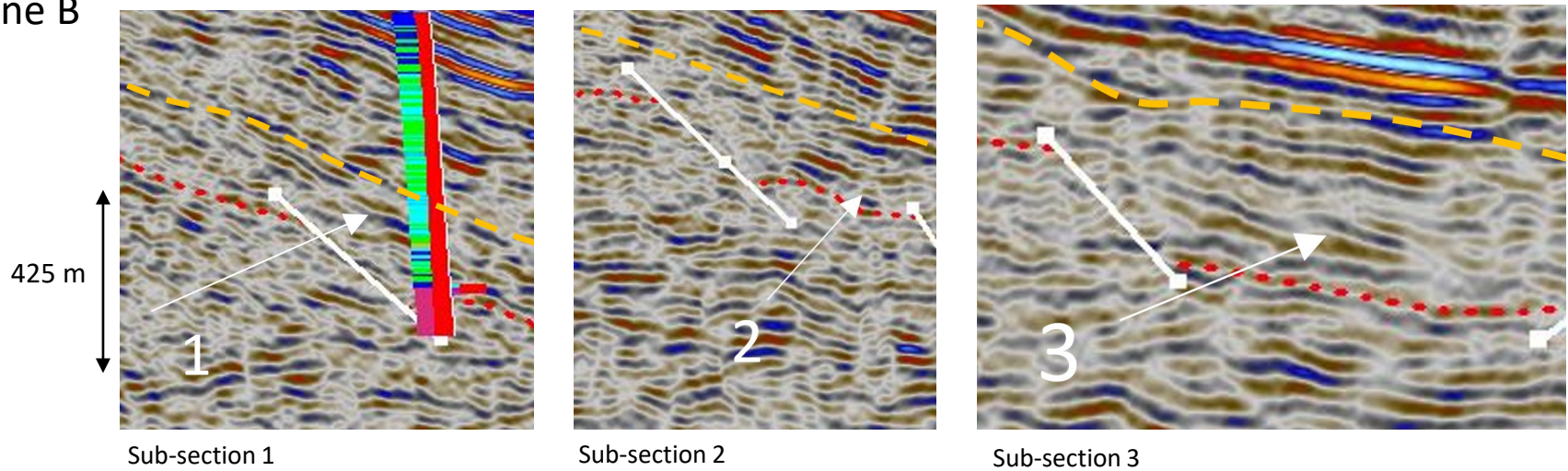
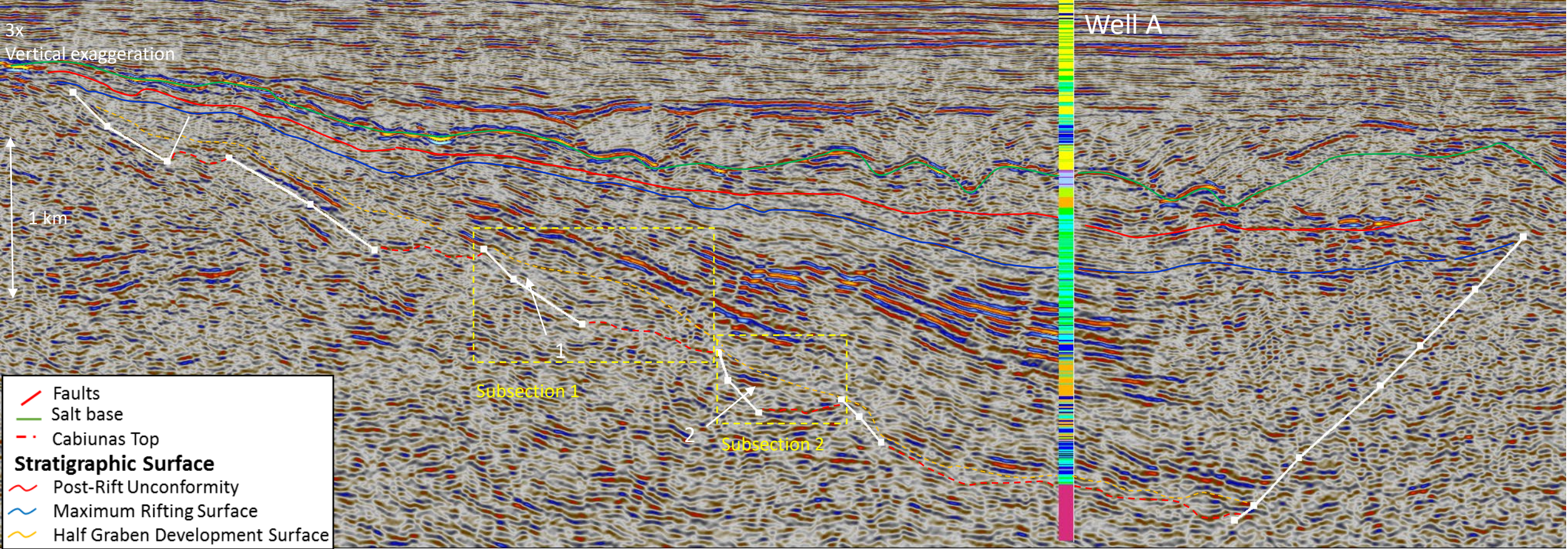


Fig 5B

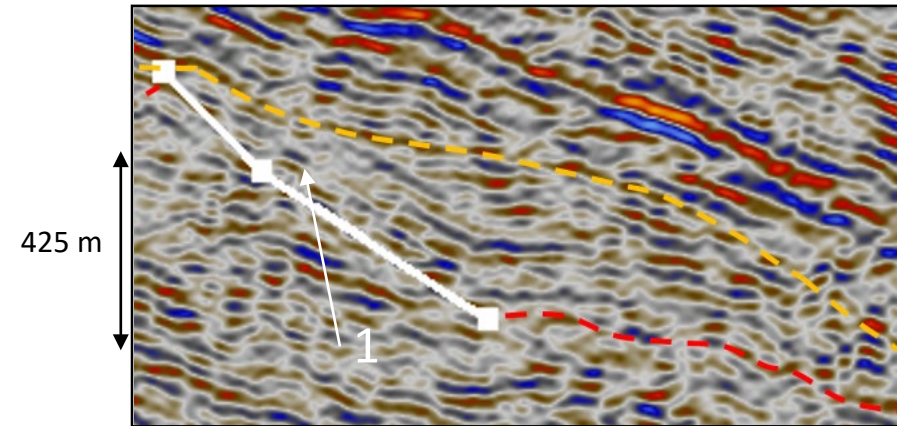
Seismic Line B



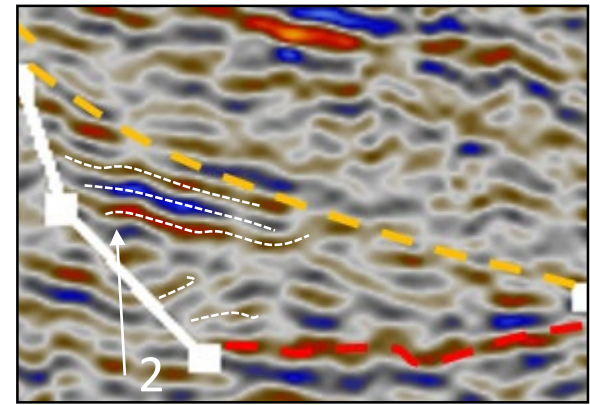


Seismic Line C

Fig 5C



Sub-section 1



Sub-section 2

Legend

- |   |   |
|---|---|
|  Silty-argillite                 |  Calcilutite |
|  Conglomerate                    |  Calcarenite |
|  Shale                           |  Coquina     |
|  Arenite                         |  Gypsum/Salt |
|  Basalt/diabase<br>Cabiunas Form |  Marl        |

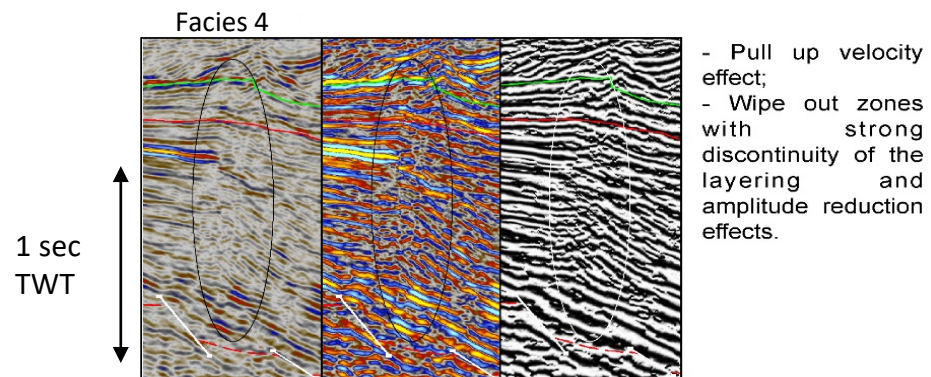
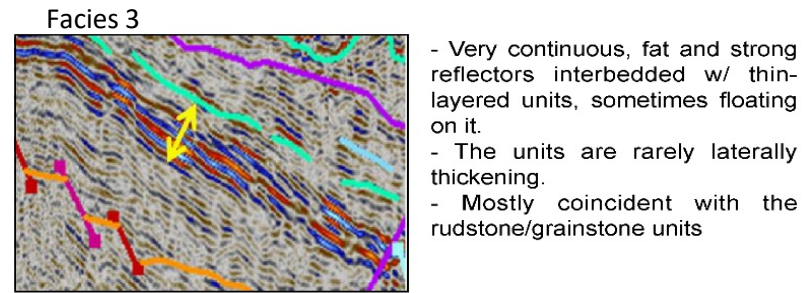
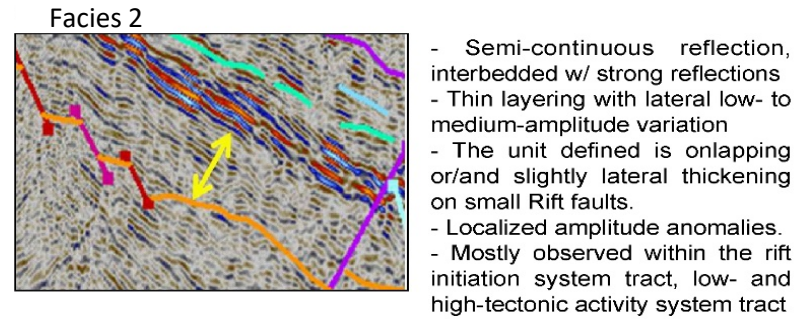
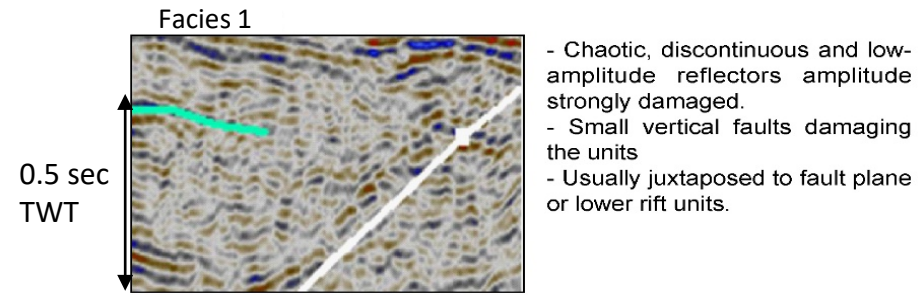
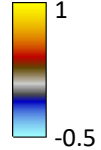
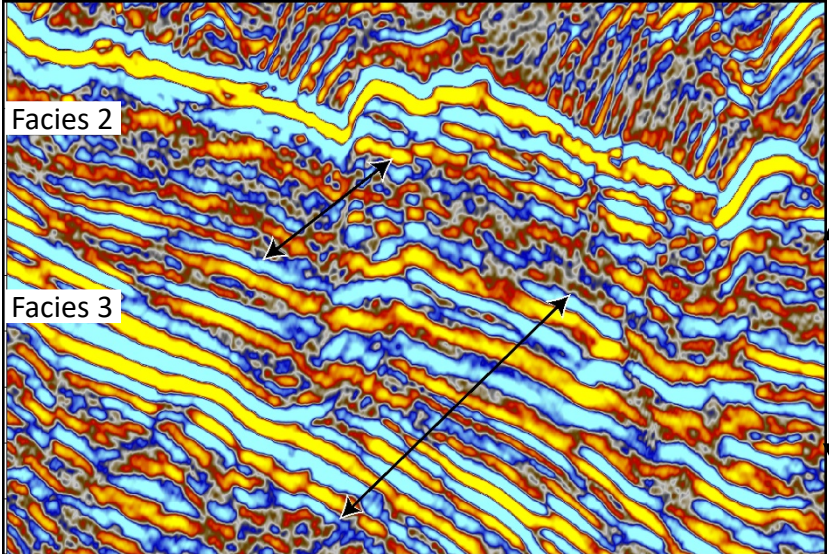


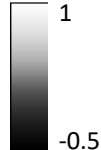
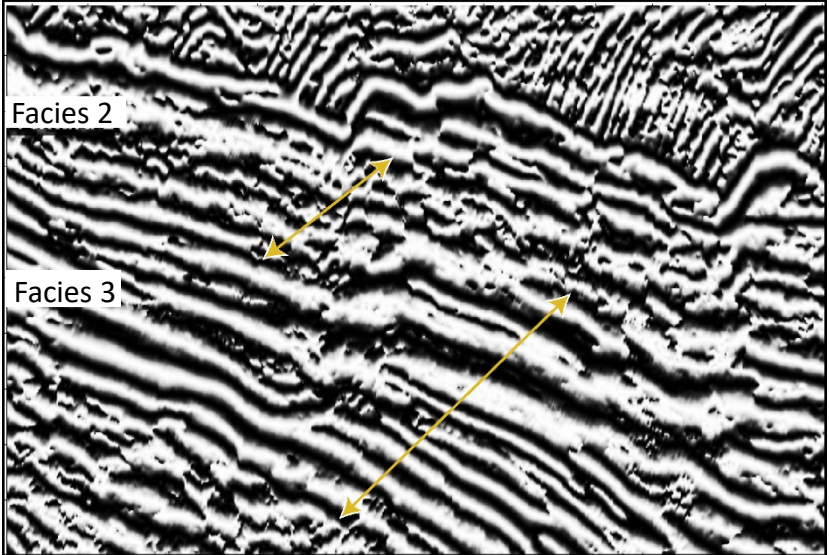
Figure 6

Seismic Line A



500 m

A



B

Fig. 7

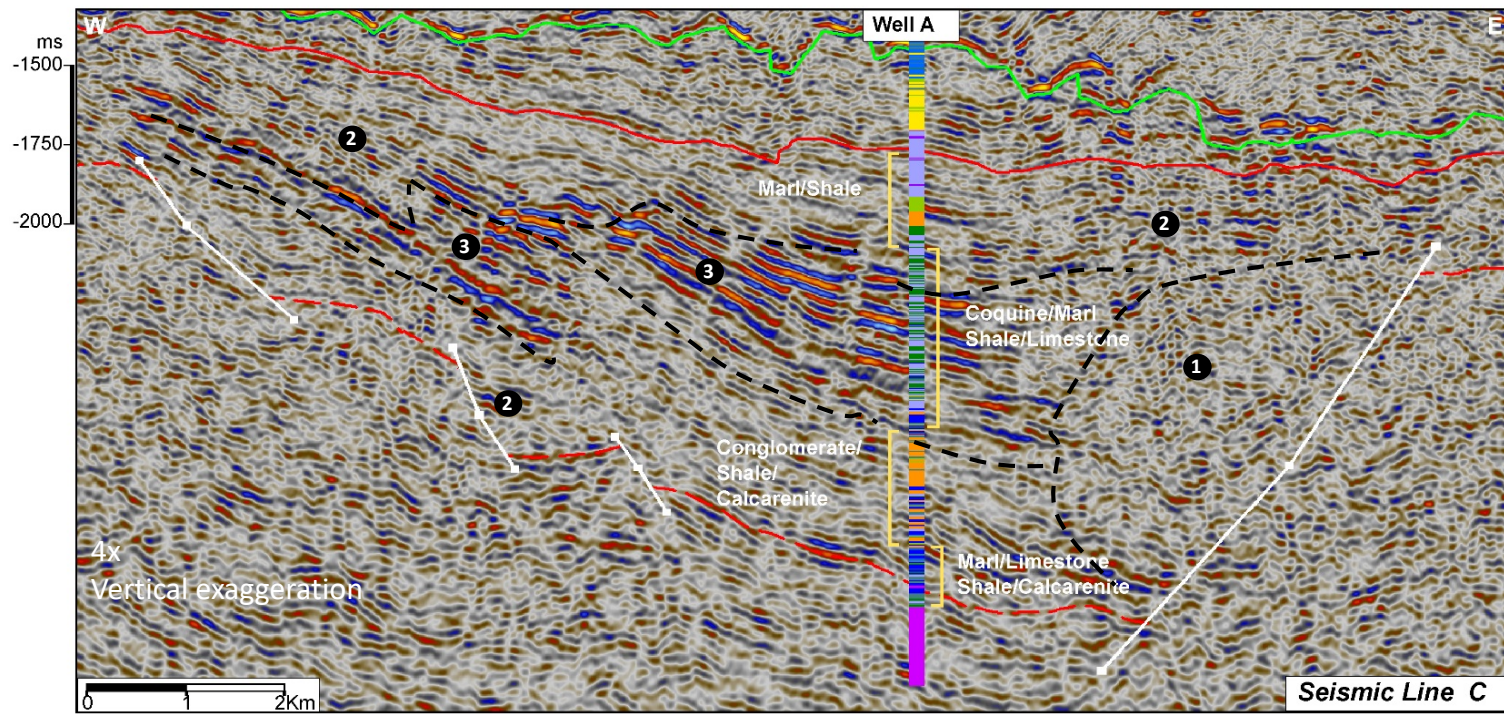


Fig 8

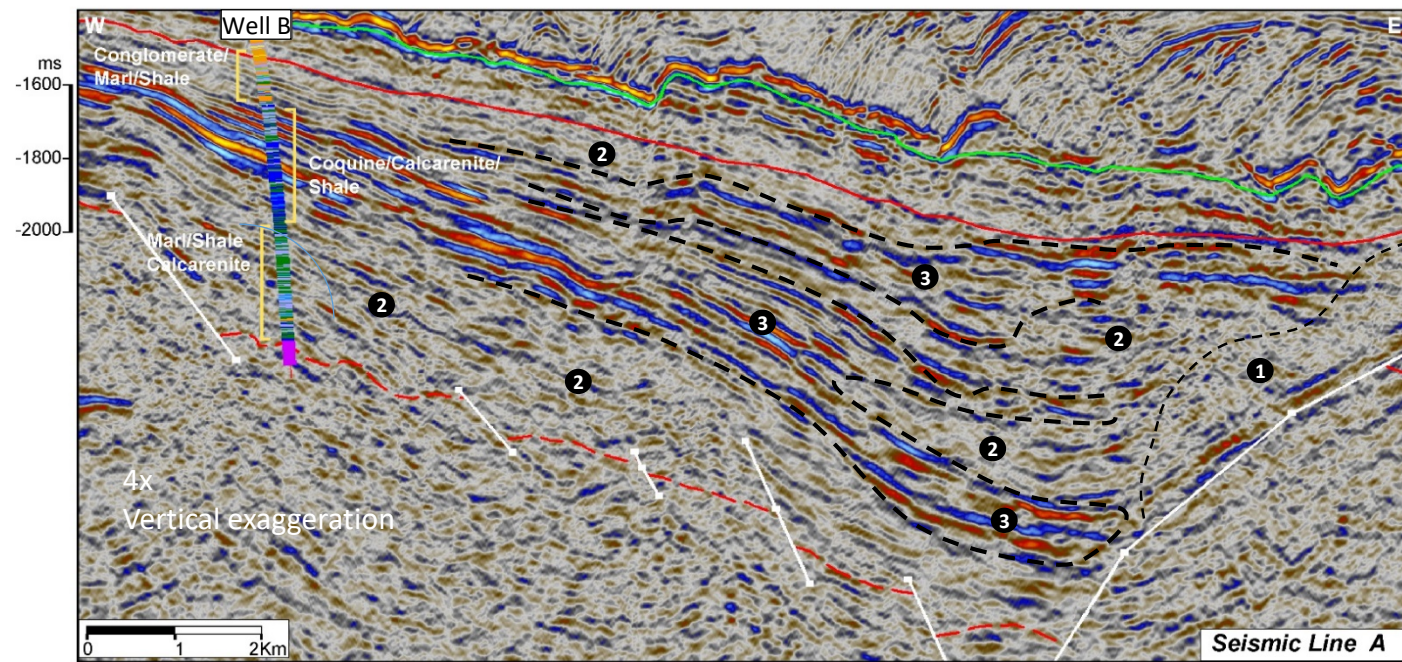


Fig 9

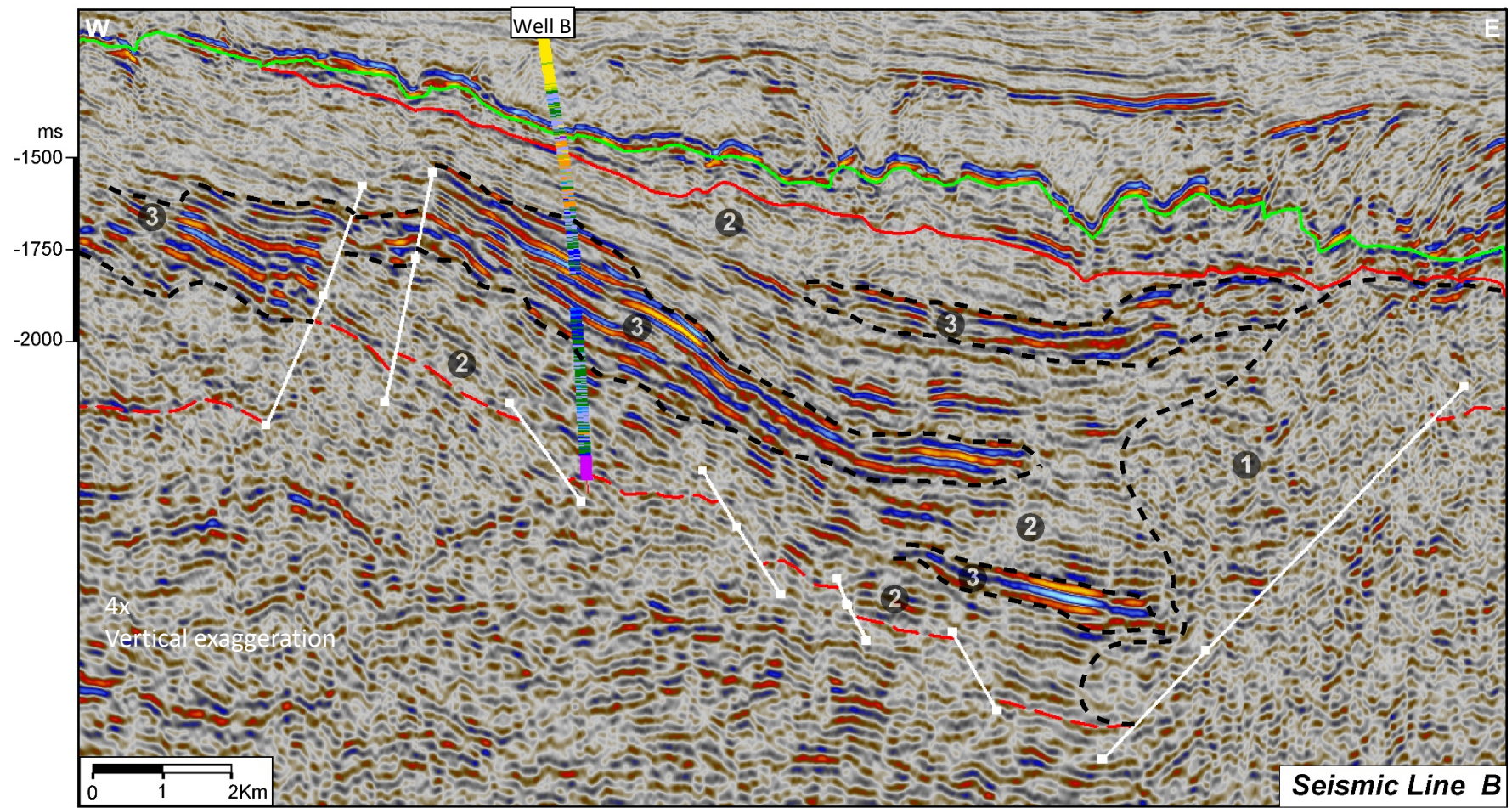
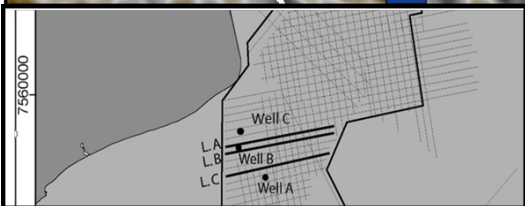
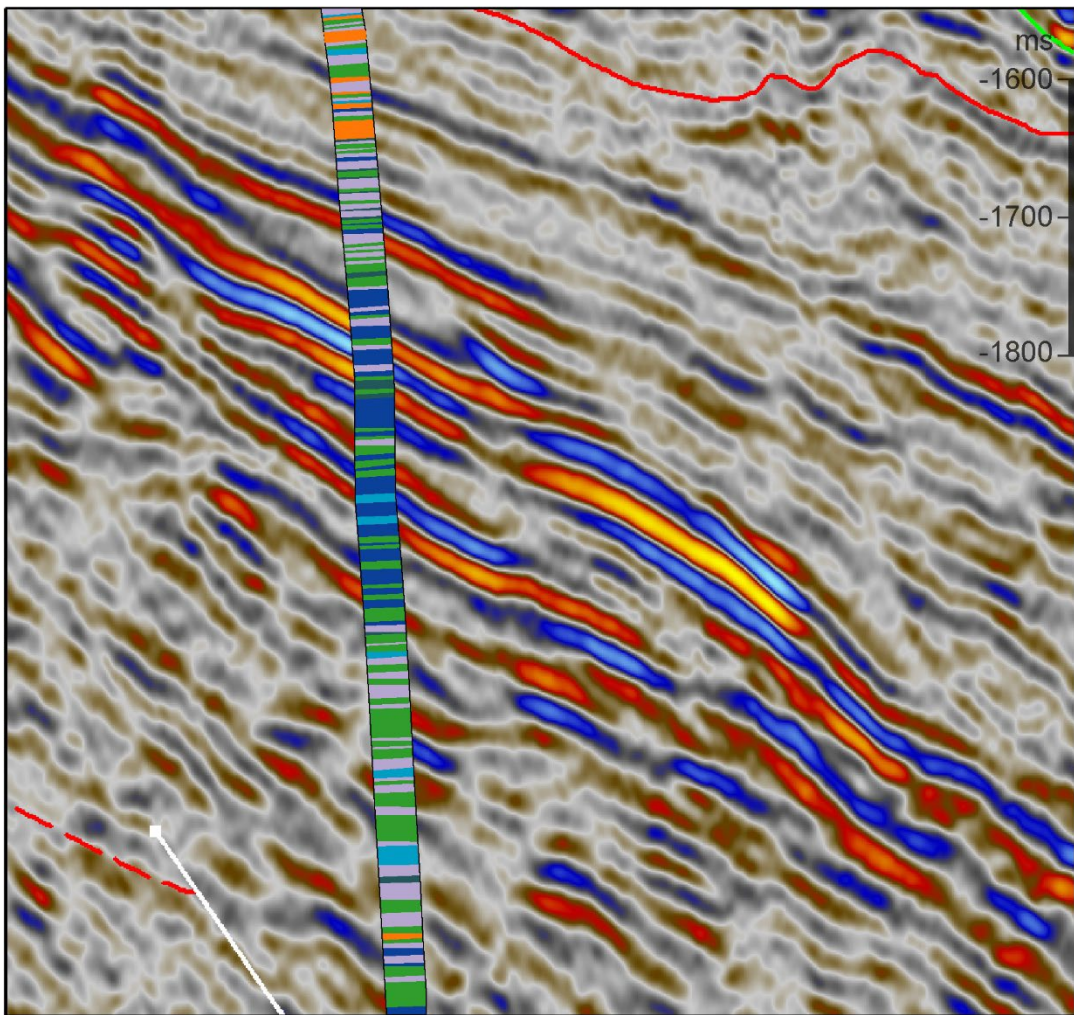


Fig 10

# Seismic Line A - Well B



## Legend

 Silty-argillite	 Calcilutite
 Conglomerate	 Calcarenite
 Shale	 Coquina
 Arenite	 Gypsum/Salt
 Basalt/diabase	 Marl

Fig 11

# Seismic Line A

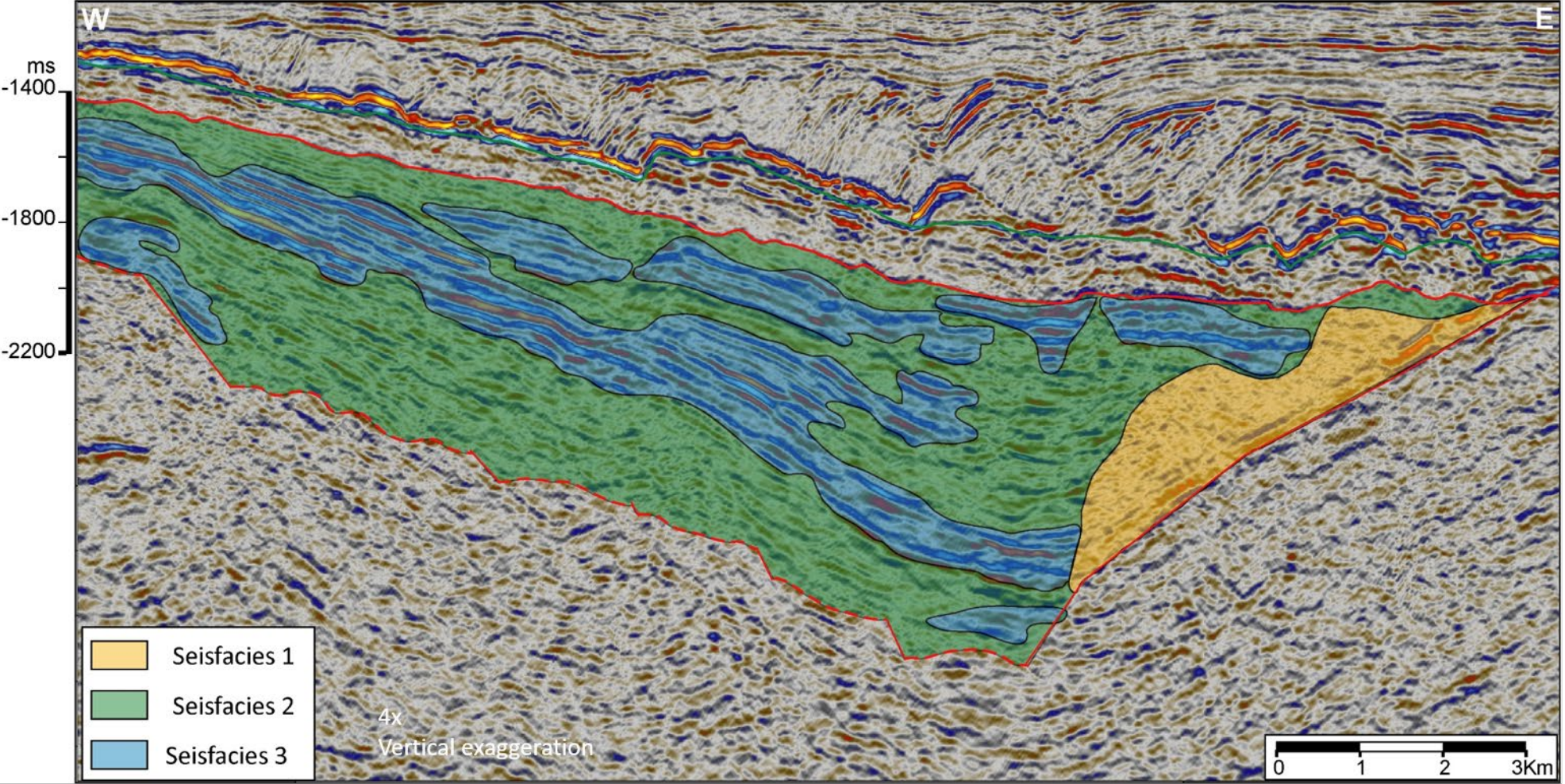


Fig 12

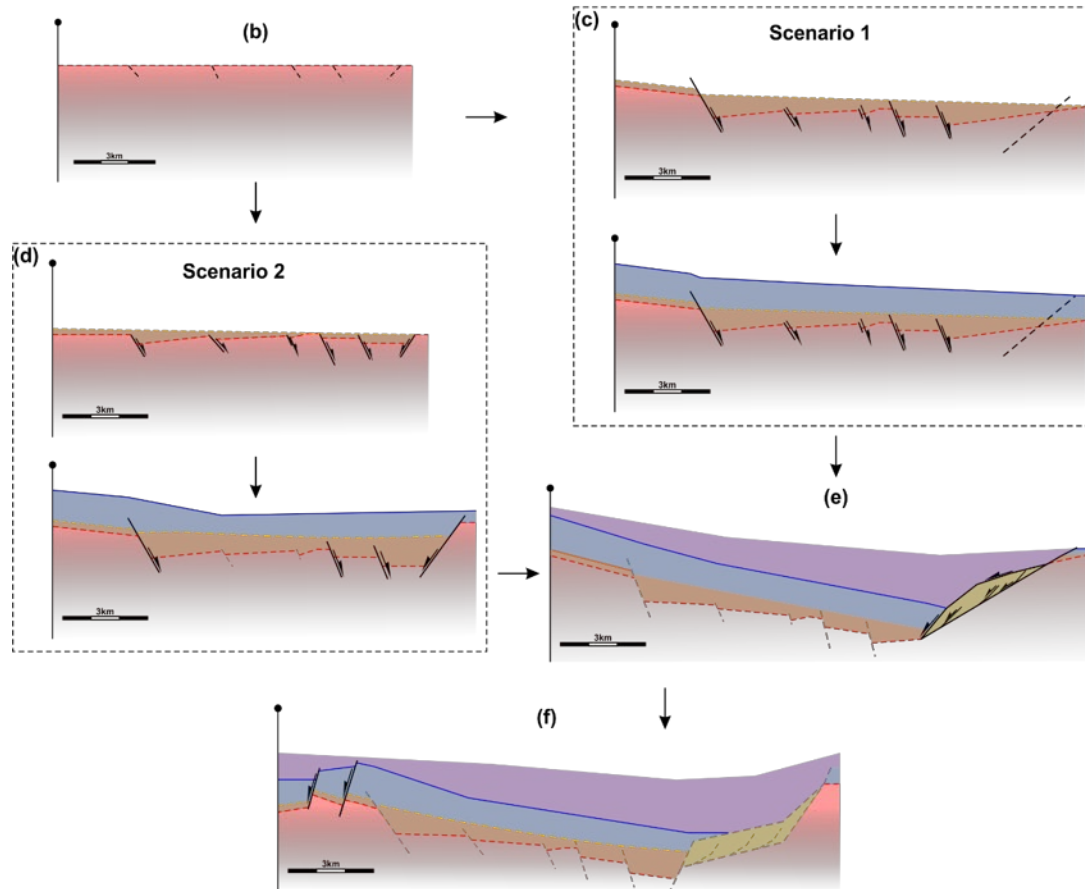
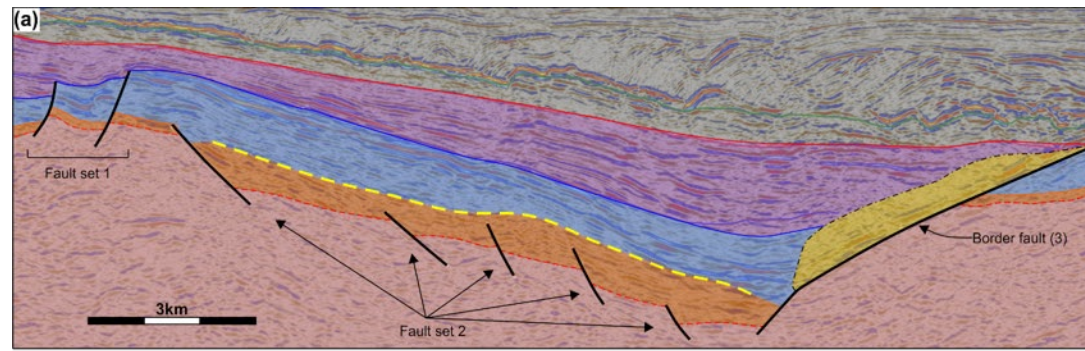


Fig 13

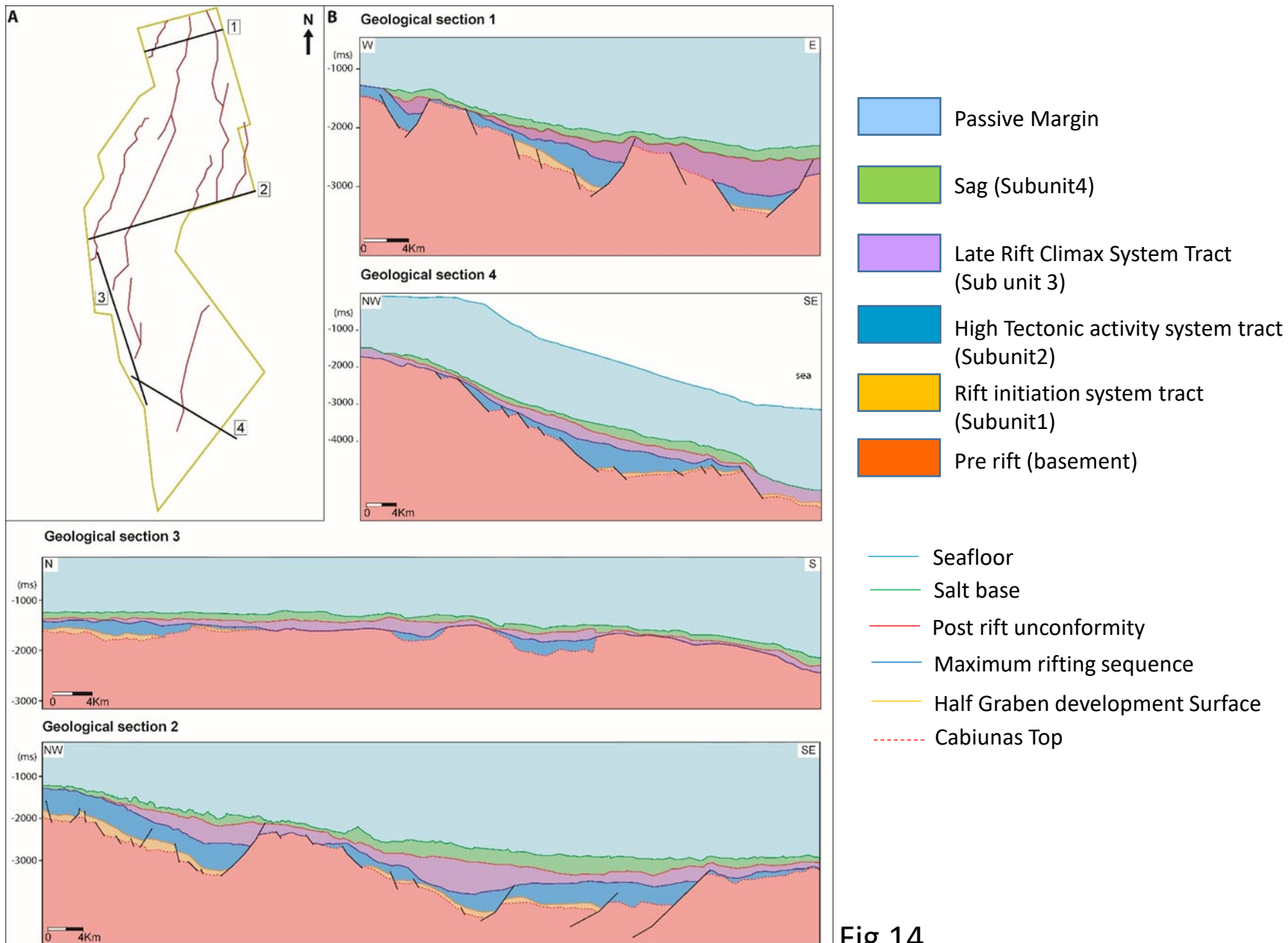


Fig 14

0

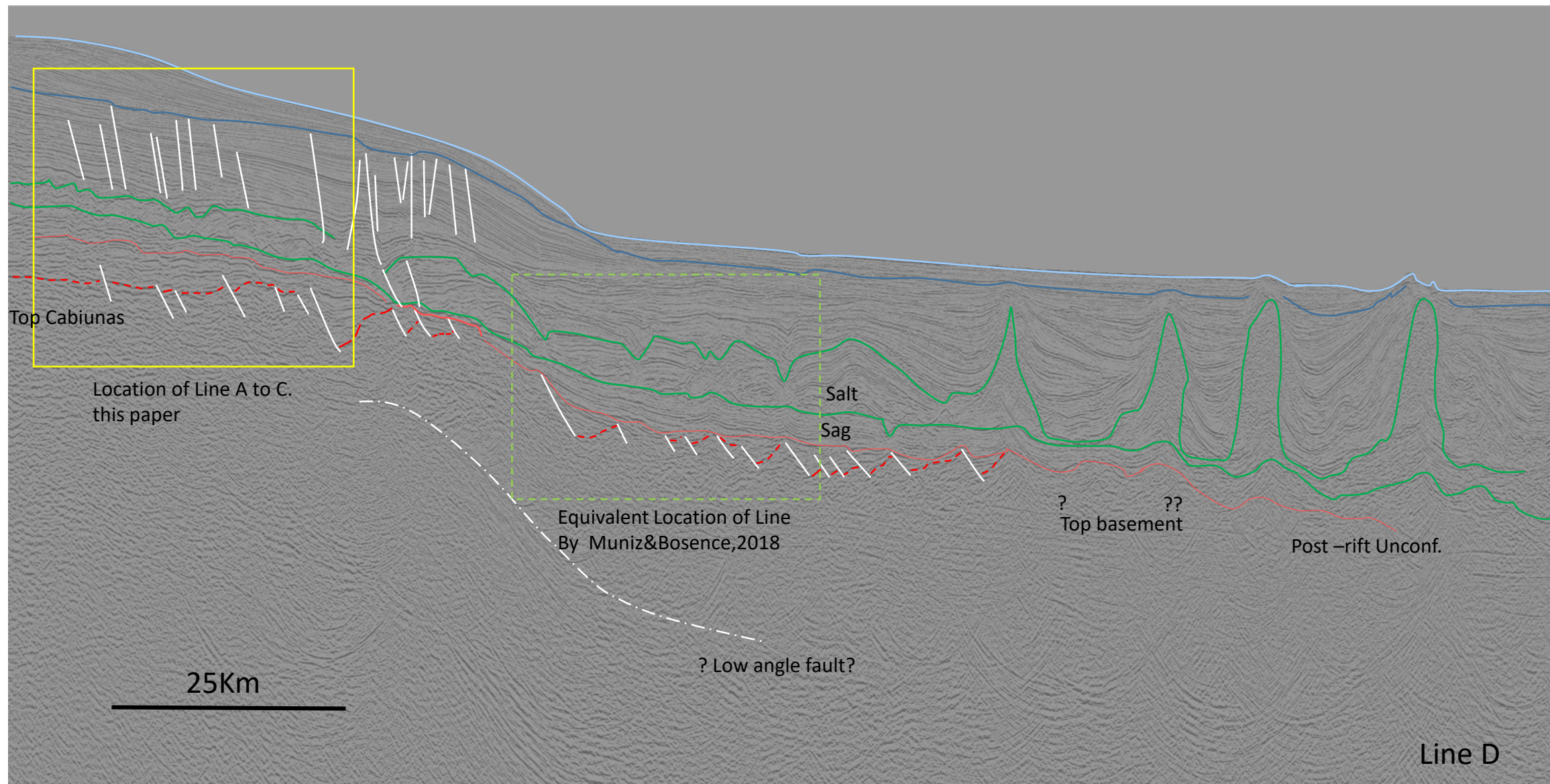


Fig 15